JOURNAL OF GEOPHYSICAL RESEARCH, VOL. 90, NO. D3, PAGES 5547–5566, JUNE 20, 1985

Trace Gas Trends and Their Potential Role in Climate Change

V. RAMANATHAN, R. J. CICERONE, H. B. SINGH,[1] AND J. T. KIEHL

National Center for Atmospheric Research, Boulder, Colorado

This study examines the potential climatic effects of the radiatively active trace gases that have been detected in the atmosphere including chlorofluorocarbons, chlorocarbons, hydrocarbons, fluorinated and brominated species, and other compounds of nitrogen and sulfur, in addition to CO_2 and O_3. A one-dimensional radiative-convective model is used to estimate trace gas effects on atmospheric and surface temperatures for three cases: (1) modern day (1980) observed concentrations are adopted and their present trends are extrapolated 50 years into the future. These projections are based on analyses of observed trends and atmospheric residence times; (2) the preindustrial to present increase in CO_2 and other trace gases are inferred from available observations; (3) a hypothetical increase of 0–1 ppbv is considered to provide insights into the radiative processes. Trace gases other than CO_2 are shown to be potentially as important as CO_2 for long-term climate trends. The relative importance of the 30 or so trace gases included in this study depends on the problem under consideration. The inferred CO_2 increase from preindustrial to the present causes an equilibrium warming of the model surface by 0.5 K, which is amplified by 50% by CH_4, $CFCl_3$ (F11), CF_2Cl_2 (F12), and tropospheric ozone. For the projected increase from year 1980 to 2030, the other trace gases amplify the estimated CO_2 warming of 0.7 K by about 110%: $CFCl_3$, CF_2Cl_2, ozone, and CH_4 each contribute in the 0.1–0.2 K range followed by N_2O, $CHClF_2$ (F22), CH_3CCl_3, and CCl_4 in the 0.03–0.1 K range. Finally, on a per ppb basis, about 12 trace gases are identified to be important: $CBrF_3$, C_2F_6 (F116), CHF_3, and CF_3Cl (F13) have greenhouse effects comparable to those of $CFCl_3$ (F11) and CF_2Cl_2 (F12). The narrow-band overlap treatment and the accurate spectral and angular integration techniques employed in the present radiation model enable quantitative interpretation of the differences between various published estimates for the greenhouse effects of $CFCl_3$ and CF_2Cl_2. For the projected trace gas increase, we compute the stratospheric O_3 change by employing a photochemical model coupled to the radiative-convective model. The O_3 change cools the stratosphere and the magnitude of the cooling is as large as that due to the projected CO_2 increase. Because of the O_3-induced stratospheric cooling and the surface warming due to the greenhouse effect, the trace gas effects on climate are virtually indistinguishable from those of CO_2.

1. INTRODUCTION

The release of chemicals into the atmosphere has grown greatly over the last 50 years. Increased reliance on synthetic chemicals, deforestation, biomass burning, and fossil fuel combustion have all contributed to the observed perturbations of trace chemicals in the atmosphere. One of the important potential consequences of this chemical change is an alteration of the earth's climate because trace chemicals modify the radiation energy balance of the earth-atmosphere system. To date, the climatic effects of future levels of CO_2 have received the most attention [e.g., see *National Research Council*, 1982, 1983; *World Meteorological Organization*, 1983]. However, from the studies summarized by the *World Meteorological Organization* [1982*a*] as well as subsequent publications [*Chamberlain et al.*, 1982; *Alexandrov et al.*, 1981; *Ramanathan*, 1982; *Hansen et al.*, 1982; *Wuebbles*, 1983*a*], it can be inferred that the combined effects of the other trace gases is to warm the surface-troposphere system and the magnitude of this warming in the future can potentially be as large as the warming due to projected increases in CO_2.

The study of climatic effects of other trace gases poses certain special problems. The difficulty encountered in examining the effects of trace gases other than CO_2 arises because they perturb the radiation energy balance of the earth/troposphere/stratosphere system in a number of ways: (1) some of the trace gases (e.g., $CFCl_3$, CF_2Cl_2, and CH_4) have strong infrared bands in the 5- to 20-μm wavelength region, which enhance the atmospheric opacity and contribute to the greenhouse effect [e.g., *Ramanathan*, 1975; *Wang et al.*, 1976]; (2) addition of chemicals, such as CO and NO, even if by themselves they are not radiatively important, can alter the chemistry of the background troposphere, which in turn can perturb the radiatively important gases, such as O_3 and CH_4 [*Hameed et al.*, 1980]; (3) the IR cooling due to the increase in several of the gases perturbs the stratospheric temperature, so that the middle stratospheric chemistry is altered appreciably through temperature-dependent reaction rates [*Boughner and Ramanathan*, 1975]. The net effect of these chemical-radiative interactions is a substantial perturbation of the stratospheric ozone concentrations, which in turn modulates the solar and IR fluxes to the troposphere. A summary of our current understanding of the above issues can be found by the *World Meteorological Organization* [1982*a*], which also gives a lengthy compilation of published studies on the problem hence these earlier studies will not be reviewed here.

The potential importance of the other trace gases provides the primary motivation for the present study, which attempts to examine the climatic effects of most (if not all) of the anthropogenic trace gases. The major objectives of the present study are given below in the order in which they are discussed.

1. Characterize the trace gases, their observed abundances, known sources, and sinks in the present-day atmosphere.
2. Based on current understanding of the observed trends, estimate the future concentrations of trace gases, including stratospheric ozone. This step, while it has numerous pitfalls

[1] Also at SRI International, Menlo Park, California.

Paper number 5D0059.
0148-0227/85/005D-0059$05.00

TABLE 1*a*. Estimates of the Abundance of Trace Chemicals in the Global Atmosphere of 1980 and 2030

Chemical Group	Chemical Formula	Dominant Source*	Dominant Sink*	Estimated Average Residence Time (τ_i), years	Year 1980 Global Average Mixing Ratio, ppb†	Year 2030 Probable Global Average Concentration, ppb		Remarks (also see text for details)
						Best Estimate	Possible Range	
Carbon dioxide	CO_2	N,A	O	2	339×10^3	450×10^3		Based on a 2.4% increase over the next 50 years
Nitrogen compounds	N_2O	N,A	S(UV)	120	300	375	350–450	Combustion and fertilizer sources
	NH_3	N,A	T	0.01	<1	<1		Concentration variable and poorly characterized
	$(NO + NO_2)$	N,A	T(OH)	0.001	0.05	0.05	0.05–0.1	Concentration variable and poorly characterized
		N,A	T(O,OH)?	1(?)	0.52	0.52		Sources and sinks largely unknown
Sulfur compounds	CSO	N,A	T	1(?)	<0.005	<0.005		Sources uncharacterized
	CS_2	A(?)	T(OH)	0.001	0.1	0.1	0.1–0.2	Given the short lifetime the global presence of SO_2 is unexplained
	SO_2	N	T(OH)	0.001	<0.05	<0.05		
	H_2S	A	I	>500	0.07	0.24	0.2–0.31	Aluminum industry a major source
Fully fluorinated species	CF_4 (F14)	A	I	>500	0.004	0.02	0.01–0.04	Aluminum industry a major source
	C_2F_6 (F116)	A	I	>500	0.001	0.003	0.002–0.05	
	SF_6	A	S(UV),I	400	0.007	0.06	0.04–0.1	All chlorofluorocarbons are of exclusive man-made origin. A number
Chlorofluoro-carbons	$CClF_3$ (F13)		S(UV)	110	0.28	1.8	0.9–3.5	of regulatory actions are pending. The nature of regulations and
	CCl_2F_2 (F12)	A	T(OH)	20	0.06	0.9	0.4–1.9	their effectiveness would greatly affect the growth of these
	$CHClF_2$ (F22)	A	S(UV)	65	0.18	1.1	0.5–2.0	chemicals over the next 50 years.
	CCl_3F (F11)	A	S(UV)	380	0.005	0.04	0.02–0.1	
	CF_3CF_2Cl (F115)	A	S(UV)	180	0.015	0.14	0.06–0.3	
	$CClF_2CClF_2$ (F114)	A	S(UV)	90	0.025	0.17	0.08–0.3	
	CCl_2FCClF_2 (F113)	A	N(O)	1.5	0.6	0.6	0.6–0.7	Dominant natural chlorine carrier of oceanic origin
Chlorocarbons	CH_3Cl	N	T(OH)	0.6	0.03	0.2	0.1–0.3	A popular reactive but nontoxic solvent
	CH_2Cl_2	A	T(OH)	0.7	0.01	0.03	0.02–0.1	Used for manufacture of F22; many secondary sources also exist
	$CHCl_3$	A	S(UV)	25–50	0.13	0.3	0.2–0.4	Used in manufacture of fluorocarbons; many other applications as well
	CCl_4	A	T(OH)	0.4	0.03	0.1	0.06–0.3	A major chemical intermediate (global production = 10 tg/yr); possibly toxic
	CH_2ClCH_2Cl	A	T(OH)	8.0	0.14	1.5	0.7–3.7	Nontoxic, largely uncontrolled degreasing solvent
	CH_3CCl_3	A	T(OH)	0.02	0.005	0.01	0.005–0.02	Possibly toxic, declining markets because of substitution to CH_3CCl_3
	C_2HCl_3	A	T(OH)	0.5	0.03	0.07	0.03–0.2	Possibly toxic, moderate growth due to substitution to CH_3CCl_3
	C_2Cl_4	A	T(OH)	1.7	0.01	0.01	0.01–0.02	Major natural bromine carrier
Brominated and iodated species	CH_3Br	N	S(UV)	110	0.001	0.005	0.003–0.01	Fire extinguisher
	$CBrF_3$ (F13B1)	A	T(OH)	0.4	0.002	0.002	0.001–0.01	Major gasoline additive for lead scavenging; also a fumigant
	CH_2BrCH_2Br	A	T(UV)	0.02	0.002	0.002		Exclusively of oceanic origin
	CH_3I	N	T(OH)	5–10	1650	2340	1850–3300	A trend showing increase over the last 2 years has been identified
Hydrocarbons, CO, H_2	CH_4	N	T(OH)	0.3	0.8	0.8	0.8–1.2	Predominantly of auto exhaust origin
	C_2H_6	A	T(OH)	0.3	0.06	0.1	0.06–0.16	No trend has been identified to date
	C_2H_2	N,	T(OH)	0.03	0.05	0.05	0.05–0.1	No trend has been identified to date
	C_3H_8	N,A	T(OH)	0.3	90	115	90–160	No trend has been identified to date
	CO	N,A	T(SL,OH)	2	560	760	560–1140	
	H_2	N	T(UV, SL,O)	0.1–0.3	F(Z)‡	12.5%		A small trend appears to exist but data are insufficient
Ozone	O_3 (Tropospheric)	N	T(OH,UV)	0.001	0.2	0.2		Secondary products of hydrocarbon oxidation
Aldehydes	HCHO	N	T(OH,UV)	0.001	0.02	0.02		1980 concentration estimated from theory
	CH_3CHO							

*N, natural; A, anthropogenic; O, oceanic; S, stratosphere; UV, ultraviolet photolysis; T, troposphere; OH, hydroxyl radical removal; I, ionospheric and extreme UV and electron capture removal; SL, soil sink.

†These concentrations are integrated averages; for chemicals with lifetimes of 10 years or less, significant latitudinal gradients can be expected in the troposphere; for chemicals with extremely short lifetimes (0.001–0.3 years) vertical gradients may also be encountered.

‡Varies from 25 ppbv at the surface to about 70 ppbv at 9 km. The concentration was increased uniformly by the same percentage from the surface to 9 km.

is necessary for the discussions concerning the relative importance of the various trace gases.

3. From observational records and other considerations, infer the preindustrial concentrations of trace gases.

4. Estimate the radiative effects of the trace gases and their potentials for climate changes.

5. Clarify the sources for differences and discrepancies between published estimates for the trace gas radiative effects.

First, some comments are in order on the scientific necessity of this study because several papers have been published on the trace gas effects. None of the previous studies have included all of the trace gases included in this study. The present study uses new laboratory spectroscopic data made available subsequent to the earlier studies; the present study relies heavily on observed concentrations and trends for the trace gases as opposed to the hypothetical concentrations and increases assumed in most of the earlier studies. The *Lacis et al.* [1981] study did use observed trends but was restricted to only the effects of chlorofluorocarbons (CFC's), CH_4, and N_2O. *Chamberlain et al.* [1982] included the direct effects of most of the trace gases considered in this study, but inferred the temperature changes from the radiative flux change at the surface instead of the changes to the surface-troposphere system. It is the radiative flux change to the surface-troposphere system that governs the surface temperature change [*Manabe and Wetherald*, 1967; *Ramanathan*, 1981, 1982; *Hansen et al.*, 1982]. Furthermore, all of the above studies ignore stratospheric ozone changes due to CFC's.

For estimating their present-day radiative effects, we adopt the observed concentrations as of 1980. With respect to projected increases, we extrapolate the present-day trends to 50 years into the future. This procedure enables us to determine the relative importance of the various trace gases. Furthermore, we examine quantitatively the validity of the optically thin approximation, an important issue because this approximation is employed by all studies to treat the radiative effects of trace gases other than CO_2, O_3, N_2O, and CH_4.

For the purposes of this study, the word "climate" refers to surface/troposphere/stratospheric temperatures. The temperature changes are computed from a one-dimensional radiative-convective model described by *Ramanathan* [1981]. The radiative-convective model provides a convenient framework for examining the other trace gas effects, even though it ignores several important feedback processes arising from atmospheric circulation, oceans, and the cryosphere (e.g., ice-albedo feedback). Numerous one-, two-, and three-dimensional climate model calculations have estimated the surface warming due to doubled CO_2 (see summaries by the *National Research Council* [1982, 1983], among several others). Furthermore, the radiative effects of the other trace gases (with the exception of stratospheric ozone changes) are very similar to that of CO_2. Hence one-dimensional model estimates for the surface warming effects of the other trace gases and that of CO_2 (provided both are performed with the same model) can be used to scale the effects for the more realistic general circulation models (GCM), since numerous GCM estimates for the CO_2 effects are currently available.

2. Observed and Projected Concentrations of Trace Gases

The earth's atmosphere currently contains trace gases with atmospheric lifetimes that vary from much less than an hour to several hundred years. The abundance of trace gases is therefore dictated as much by their removal rates as by the growth in sources. From a viewpoint of global climate effects, species with extremely short lifetimes are unlikely to play an important direct role. To project the concentration of each species to year 2030, we have used a knowledge of the following: (1) recent (1980) atmospheric concentration and recent trend data if any; (2) nature of sources (man-made, natural, etc.), relative strengths or budget for each gas; (3) growth in natural as well as man-made sources due to projected human activities over the next 50 years; and (4) atmospheric lifetimes of each species.

TABLE 1*b*. Assumed Preindustrial (Year 1880) Concentrations of the Trace Gases

Trace Gas	Concentration
CO_2	270 ppm
CH_4	1.15 ppm
N_2O	0.285 ppm
Tropospheric O_3	−12.5%*
Stratospheric O_3	Same as present-day values
CFC11 and 12	0.
CCl_4	0.
All others	0.

*O_3 concentration is altitude dependent. Uniformly smaller at all altitudes from 0 to 12 km by 12.5%.

In what follows, we emphasize radiatively important gases. Table 1*a* briefly describes the lifetimes, dominant sources, and sinks of trace chemicals that have been identified in the global atmosphere. Many of these properties were listed earlier in an extensive review of scientific literature [*World Meteorological Organization*, 1982*b*]. For a large number of species where reaction with hydroxyl radical (OH) is the principal removal mechanism, lifetimes are estimated using an average OH concentration of 7×10^5 molecules/cm^3 and an average global atmospheric temperature of 265 K. While uncertain, this OH average is consistent with the budgets of CH_3CCl_3, CO, and ^{14}CO [*Volz et al.*, 1981]. For species with lifetimes greater than 20 years in Table 1*a*, removal is largely due to photolytic decomposition in the stratosphere. For all of the chlorofluorocarbons in Table 1*a*, lifetimes are determined based only on stratospheric photolysis from the computations of *Wuebbles* [1981] and those summarized by the *World Meteorological Organization* [1982*b*]. Only oxygenated species (O_3, aldehydes) and CH_3I absorb UV light in the troposphere ($\lambda > 290$ nm). The fully fluorinated species are not decomposed by UV light even in the stratosphere. Their destruction by and large would occur in the mesosphere and ionosphere from absorption of Lyman alpha and Lyman beta radiation at altitudes above 70 km [*Cicerone*, 1979]. The lifetime of fully fluorinated organics (Table 1*a*) can be in the 500- to 1000-year range. Hydrogen is the only species in Table 1*a* where microbial action at soil surfaces provides the major removal process. Ozone destruction also occurs on all surfaces (e.g., soil, water, and snow), but the mechanism of this destruction process is not known.

In addition to providing source, sink, and lifetime information, Table 1*a* also presents global average concentrations of species for the atmosphere of year 1980. These data are based on actual measurements that have already been summarized in some detail [*World Meteorological Organization*, 1982*b*].

It must be remembered that for species with lifetimes of less than 10 years, significant horizontal (latitudinal) gradients can exist. As an example, the ratio of northern to southern hemis-

pheric average concentration is about 1.4 for CH_3CCl_3 ($\tau_l = 8$ years) and >2 for C_2Cl_4 ($\tau_l = 0.5$ year). For short-lived species ($\tau_l < 0.3$ year), vertical gradients can also be expected. These gradients have been taken into consideration, based on available information, in developing the global averages shown in Table 1*a*.

The year 2030 concentrations are projected to develop a standard set of conditions, but a probable range is also included. The year 2030 "best estimates" in Table 1*a* thus constitute the "standard set." The range of likely variability associated with this standard set is also presented in Table 1*a*.

In the following sections we discuss the information that was utilized in developing the year 2030 projections. The year 1980 characterization is based exclusively on atmospheric measurements.

2.1. *Carbon Dioxide*

The CO_2 concentrations in the atmosphere have been measured to be increasing at a rate of approximately 1.5 ppm/yr (see Figure 1.2 of the *National Research Council* [1983]). Fossil fuel combustion is believed to be a major contributor to this increase. Over the past decades, CO_2 release rates due to combustion have increased at a rate of about 4.3%/yr. A recent analysis [*Rotty and Marland*, 1980] supports a 2.4%/yr increase in CO_2 emissions over the next 50 years. Only a fraction ($\approx$50%) of this input is expected to remain airborne. Based on this analysis, *Wuebbles* [1981] described the CO_2 concentration in ppm empirically.

$$[CO_2] = 330.0e^{0.0056(t-1975)} \qquad 1975 \leq t \leq 2100$$

The CO_2 concentration of year 2030 is computed to be 450 ppm. This projected concentration is consistent with available scenarios based on more detailed considerations of energy policies and the sources and sinks for CO_2 [e.g., *Smagorinsky*, 1983, p. 278].

2.2. *Chlorofluorocarbons (CFC's)*

These chemicals came into major use in the 1960's and initially exhibited a rapid growth (10–15%/yr). The most important CFC's to date have been CF_2Cl_2 (F12 or CFC12) and $CFCl_3$ (F11 or CFC11). The global emissions of the major CFC's (F12 and F11) actually declined somewhat from the mid-1970's through 1982 [*Chemical Manufacturer's Association*, 1983]. Part of this decline may be attributed to a ban on some nonessential usages (e.g., spray cans) of CFC's and due to adverse economic conditions that have prevailed in several industrial nations during this time. CFC emissions increased sharply in 1983. Data for $CFCl_3$ and CF_2Cl_2 have been presented by *Logan et al.* [1981] and *Cunnold et al.* [1983*a*, *b*]. The use of CFC's in other more essential industries and in previously less industrialized nations (e.g., refrigeration) is expected to grow. We estimate that a 3%/yr growth rate for all of the relatively inert CFC's, i.e., F11, F12, and $C_2Cl_3F_3$ (F113), $C_2Cl_2F_4$ (F114), C_2ClF_5 (F115), and C_2F_6 (F116), is a reasonable scenario. The range of concentrations shown in Table 1*a* is established based on a 0–5%/yr growth. For $CHClF_2$ (F22), less severe controls are anticipated, since 60% of the emitted amount could be removed in the troposphere. A 5% growth rate with a 3–7%/yr range is used for computations presented in Table 1*a*.

2.3. *Chlorocarbons*

All chemicals (except carbon tetrachloride) in this category have atmospheric residence times of less than 10 years. Because of the toxic nature of many of these chemicals [*Surgeon General*, 1980], a rapid growth of emissions cannot be expected. Also, because of relatively fast removal rates, a dramatic buildup of these in the global atmosphere is not likely.

Methyl chloride (CH_3Cl) is the most abundant natural chlorine carrier; it appears to arise mostly from the world's oceans [*Lovelock*, 1975; *Rasmussen et al.*, 1980; *Singh et al.*, 1983*b*], although relatively small man-made sources are known to exist [*National Academy of Sciences/National Research Council*, 1976] and inadvertent release is possible due to biomass burning and/or reactions between organic matter and chlorinated water, as in rivers. Thus it is unlikely that the sources of atmospheric CH_3Cl will increase substantially, and we indicate in Table 1*a* little or no growth in its atmospheric concentration by the year 2030. It is worth noting, however, that if tropospheric OH (dominant sink for CH_3Cl) levels decrease, CH_3Cl concentrations could increase; see methane discussion below.

Methylene chloride (CH_2Cl_2), a relatively short-lived chemical, is a popular solvent which is expected to undergo rapid growth unless found to be toxic in the future. Its virtual noninvolvement in the stratosphere and its lack of toxicity assures it an excellent growth potential. On the average, a 5%/yr (range of 3–7%/yr) growth rate appears a reasonable projection. This growth rate is also consistent with the growth in the last decade [*Bauer*, 1979].

Over the last decade, the methyl chloroform (CH_3CCl_3) market has grown at a rate of about 15%/yr. Although it may make an increasing contribution to stratospheric ozone depletion, its market is expected to grow rapidly and a growth rate similar to that of CH_2Cl_2 is projected. Methylene chloride along with CH_3CCl_3 are the most likely chemicals to be used for substitution as other more toxic chemicals (e.g., C_2HCl_3, C_2Cl_4) are more severely controlled.

Carbon tetrachloride (CCl_4) is the longest lived atmospheric chlorocarbon, and its historical emission pattern is more complicated [*Singh et al.*, 1976]. Since the early 1960's, when the toxic effects of CCl_4 became evident, direct emissions virtually ceased. The present atmospheric CCl_4 concentration growth rate is between 2%/yr [*Simmonds et al.*, 1983] and 5%/yr [*Singh et al.*, 1983*a*]. Current emission levels of CCl_4 could grow at a rate of about 2% (0–3%/yr) over the next 50 years, in a manner similar to those of fluorocarbons because a large fraction of CCl_4 emitted is during its use in fluorocarbon production.

2.4. *Fully Fluorinated Species*

Three chemicals in this cateogry have been measured at enough locations to characterize global concentrations: CF_4 (F14), C_2F_6 (F116), and sulfur hexafluoride (SF_6). These three man-made species are relatively stable chemicals with atmospheric residence times over 500 years. These species are not chemically involved in atmospheric processes below about 50 km. The sources of CF_4 and C_2F_6 are not at all clear. Inadvertent emissions from carbon-electrode processing of minerals [*Cicerone*, 1979] are likely, specifically from aluminum processing [*Penkett et al.*, 1981]. Assuming a 2–3% steady growth rate of the aluminum industry over the next 50 years, the year 2030 concentrations of CF_4 and C_2F_6 are shown in Table 1*a*. Indeed, a temporal increase of about 2%/yr in CF_4 concentrations has been measured recently (R. J. Cicerone et al., unpublished manuscript, 1985). This rate of increase is less than that deduced by *Cicerone* [1979]. SF_6 is a dielectric

trend, but an upward trend in tropospheric ozone (2–8 km) seems to have occurred [*Angell and Korshover*, 1983].

Other considerations suggest that tropospheric ozone is increasing in the northern hemispheric troposphere. First, *Fishman et al.* [1979*b*] presented evidence that there is appreciable in situ photochemical production of ozone. This evidence includes the fact that ozone is more concentrated in the NH even though there should be faster uptake at the earth's surface in the NH. Also, Fishman et al. noted that there are much stronger seasonal variations in the NH production of ozone. Recent models of tropospheric chemistry that embody this theory predict that tropospheric ozone has already increased and will continue to do so, especially in the NH. Due to increases in combustion releases of NO_x, CO, H_2, and increased CH_4, *Logan et al.* [1978] calculated that tropospheric O_3 can increase greatly, even 100% in the next century, especially in the middle and upper troposphere. *Liu et al.* [1980] focused on the consequences of NO_x injections from high flying aircraft. In their view, most photochemical production of ozone occurs above the boundary layer, so direct injections by aircraft are especially effective and ground-level NO_x sources may not lead to much photochemical ozone in the free troposphere. Liu et al. calculated that a 14–30% ozone increase should have occurred in the NH middle and upper troposphere between 1970 and 1980. A more recent analysis of tropospheric ozone production by human activities is given by *Crutzen and Gidel* [1983].

To summarize the two paragraphs above, there is some observational evidence that NH tropospheric ozone has increased by 0.8–1.5%/yr since about 1967; this evidence is compelling but not conclusive. Photochemical theory applied to emission histories and projections of combustion NO_x suggests that a 1%/yr increase in NH tropospheric ozone is possible. In the SH, given the smaller anthropogenic influences, O_3 might not change at all (NH anthropogenic NO_x, a key ingredient for photochemical production of O_3, should not influence the SH). For our globally averaged radiative calculations, we will adopt an annual growth rate for tropospheric ozone of 0.25%/yr, although values from zero to 1.5%/yr appear possible, at least for the NH. A nominal 40 ppb of tropospheric ozone, for example, becomes 45 ppb in the year 2030 with a 0.25%/yr growth rate; a 1%/yr growth rate would result in 64 ppb in 2030. Note that we do not assume a constant mixing ratio with altitude in our calculations. Table 1*a* provides the adopted altitude variation in the model calculations which are based on the hemispherical, annual mean ozone data described by *Ramanathan and Dickinson* [1979].

Stratospheric ozone is also thought to be susceptible to perturbing influences, including man-made chloro- and chlorofluorocarbons, increasing CH_4 and N_2O concentrations (see below) and decreases in stratospheric temperature due to increasing CO_2. For our stratospheric ozone profile for the year 2030, we have taken the computed ozone perturbations listed in Table 2. These ozone changes were calculated with the basic chemistry model of *Cicerone et al.* [1983] with fixed-flux lower boundary conditions for N_2O, CH_3Cl, and CCl_4 but a fixed mixing ratio (1.6 ppm) for CH_4. As discussed later, the present computations account for the feedback between temperature and chemistry. A refined diurnal averaging scheme was employed; it led to less nonlinearity in the ozone-chlorine response curve than reported by Cicerone et al. The ozone change shown in Table 2 was obtained by increasing the flux of $CFCl_3$ (F11) and CF_2Cl_2 (F12) till the stratospheric mixing ratio of inorganic chlorine (ClX) reached a value of 9.4 ppb for the year 2030. A ClX value of 9.4 ppb for year 2030 results from a 3%/yr increase (1980–2030) in emissions of CF_2Cl_2, $CFCl_3$, CH_3CCl_3, $C_2Cl_3F_3$, $C_2Cl_2F_4$, CCl_4, and $CHClF_2$ (D. J. Wuebbles, private communication, 1984; also see *Wuebbles* [1983*b*]). This uniform 3% growth rate is consistent with those adopted in Table 1*a*, except that Table 1*a* shows a 2% growth rate for CCl_4 and a 5% rate for $C_2H_3Cl_3$. In order to place this slight inconsistency in proper perspective, we note that the calculated future stratospheric ClX mixing ratios depend, not only on future emissions, but also on the vertical eddy-mixing coefficient in the (one-dimensional) model. For the 1980 reference atmosphere, we took ClX = 2.5 ppb.

The ozone changes shown in Table 2 account for the feedback between temperature and chemistry. For this purpose, we iterated the temperature changes computed by the climate model (described later) with the ozone change resulting from the chemistry model. The temperature change calculations include not only the ozone changes but also the increase in all other trace gases shown in Table 1*a* (see the "Best Estimate" column). This temperature feedback reduced the computed ozone changes by a nonnegligible amount. For example, without the temperature feedback, the computed ozone change at a few of the levels are +4.2% (10 km), +5.1% (20 km), −7.3% (30 km), −45% (40 km), and −36% (44 km); these changes can be compared with those in Table 2.

Our usage of a fixed mixing-ratio lower boundary condition for CH_4 actually assumes an increasing flux of CH_4 (to maintain the fixed mixing ratio as ClX increases). A fixed-flux boundary condition for CH_4 would have led to larger ozone changes than those shown in Table 2. Beyond the year 2030, even larger ozone changes are possible [*Prather et al.*, 1984]. In the present paper, we have neglected stratospheric ozone changes due to the projected CH_4 and N_2O increases shown in Table 1*a*. It should also be stated that model calculations of ozone changes below 30 km are plagued with uncertainties. Accordingly, model results have fluctuated over the past 10 years or so [see, e.g., *National Academy of Sciences/National Research Council*, 1982].

2.7. *Methane (CH_4) and Carbon Monoxide (CO)*

The most abundant atmospheric hydrocarbon, methane, was present at about 1.65 ppm in the NH in 1980; a concentration about 6% lower characterized the SH. More relevant for our present purposes, atmospheric CH_4 concentrations are known to be increasing globally. Between early 1978 and early 1981, concentrations increased by (2 ± 0.5)%/yr as measured by *Rasmussen and Khalil* [1981] and by 1–1.5%/yr as measured by *Blake et al.* [1982]. *Ehhalt et al.* [1983] have reviewed these and other data on atmospheric methane and conclude that its concentration increased by about 0.5%/yr between 1965 and 1975 and by 1–2%/yr between 1978 and late 1980. Further, from trapped air in dated ice cores, *Craig and Chou* [1982] have deduced that CH_4 concentrations have approximately doubled in the last 350 years with a greater rate of increase in the last century. It is not clear why these increases have occurred, i.e., which of the methane sources have increased or even if the atmospheric sink of methane (oxidation by OH reaction) has decreased. Arguments for increasing sources of methane are favored by ^{13}C data [*Craig and Chou*, 1982]. Principal sources of atmospheric methane appear to be enteric fermentation in ruminant animals, release from organic-rich sediments below shallow water bodies and rice paddies, and quite possibly, production by termites and biomass burning. Also, methane re-

agent used in electrical equipment. Its concentrations are also estimated based on a 2–3%/yr growth rate.

2.5. *Nitrogen Compounds*

The most important nitrogen-containing chemical from a climatic viewpoint is N_2O. The 1980 atmospheric concentration is 301 ppb (0.8 ppb less in the southern hemisphere) as measured by *Weiss* [1981]. Contrary to many previous estimates, it is now accepted that N_2O has a very long atmospheric lifetime (> 100 years) with stratospheric photolysis the only known removal process. Microbial production in soils and oceans has been found to be a source as well as a sink of N_2O. The net contribution of soils and oceanic microbes to the atmospheric budget of N_2O is not yet clear; *Weiss* [1981] calculated that the total annual source of atmospheric N_2O is about 3×10^{12} g. Over a 4-year period (1976–1980), Weiss measured a rate of increase of 0.2%/yr for N_2O concentrations. Further, he constructed a mathematical model which used an exponentially increasing N_2O source function to fit his measurement data. More recent data (R. F. Weiss, private communication, 1984) continue to fit Weiss' mathematical model. The recent record shows more uniformity among data from measurement locations than was apparent in the 1976–1980 record. From the *Weiss* [1981] mathematical model, we estimate the year 2030 concentration to be 375 ppb and a likely range of 350–450 ppb. This range reflects the considerable existing uncertainty as to the identity of the N_2O sources most responsible for the observed N_2O concentration trend, e.g., coal combustion and microbial production of N_2O through nitrification and denitrification of inorganic nitrogen fertilizers applied to soils. Even with the recent expansion of Weiss's data base, the record is still not adequate to distinguish between these two sources (R. F. Weiss, private communication, 1984). In the future, the atmospheric residence time of N_2O could decrease if ozone concentrations decrease above 30-km altitude (Table 2); increased UV light levels just below 30 km would increase the rate of N_2O photolysis. Also, while we have adopted *Weiss*'s [1981] semiempirical method for projecting future N_2O concentrations, we note that there remain many questions about sources of atmospheric N_2O. For example, if we employ a slower rate of increase of fossil fuel combustion than did Weiss, we arrive at a reduced lower limit for N_2O in that year, i.e., 350 ppb. Further, while many studies suggest that only 1–2% of all fertilizer N is released as N_2O in the year following fertilization, much higher release rates are possible especially from fertilized organic-rich soils [*Duxbury et al.*, 1982].

Two other nitrogen-containing gases, hydrogen cyanide (HCN) and peroxyacetyl nitrate (PAN), have now been observed in the nonurban troposphere. Infrared absorption measurements with the sun as the source have shown that HCN is present in the northern hemisphere (NH), midlatitude troposphere, and the entire NH stratosphere at about 160 ppt, with little, if any, altitude gradient up to the midstratosphere. These measurements, the atmospheric chemistry and possible sources of HCN, have been discussed by *Cicerone and Zellner* [1983]. In Table 1*a* we show no increase in HCN concentration by 2030, but only because there are no data on its temporal trends and because the identities of its sources are uncertain. Similarly for PAN, we can do little more than note that it has been detected recently in the nonurban troposphere, occasionally at concentrations of 400 ppt. While there is reason to believe that its global concentrations are nonnegligible [*Singh and Salas*, 1983] and that its precursors (NO_x, ethane, and propane) might increase in the future, there is too little information to permit an estimate of PAN's future concentrations.

TABLE 2. Computed Stratospheric Ozone Changes From 1980 to 2030

Altitude	Percent Ozone Change
10	3.8
16	4.1
22	4.5
26	2.0
28	−1.2
30	−6.1
32	−13.4
34	−22.6
36	−31.1
38	−36.7
40	−37.9
44	−27.4
50	−5.4

The calculations account for the feedback between temperature and chemistry within the model stratosphere (above 10 km) and employ the chemistry model of *Cicerone et al.* [1983] and the radiative-convective model used in this study.

The other nitrogen species (NH_3 and NO_x) have extremely short lifetimes (0.5–5 days). The global distribution of these species, even for the 1980 atmosphere, is poorly characterized [*Kley et al.*, 1981]. As expected with species of such short lifetime, a great deal of variability in atmospheric levels is evident. Although anthropogenic sources of NO_x in the troposphere (auto and aircraft exhaust, high-temperature combustion, soil emissions) may double over the next 50 years, it is unclear if this change would increase the atmospheric abundance of NO_x outside the range of present uncertainty.

2.6. *Ozone*

The climatic effects of ozone change depend very strongly on whether tropospheric or stratospheric ozone is being altered [*Ramanathan and Dickinson*, 1979; *Wang*, 1982]. Hence we discuss separately the tropospheric and stratospheric O_3 trends.

Focusing first on ozone in the free troposphere (above the planetary boundary layer), there are data and theories that suggest that ozone concentrations are increasing with time. A number of investigators [*Logan*, 1982; *Angell and Korshover*, 1983; *Bojkov*, 1983] have reviewed and analyzed data from many ozone-measuring stations supported by Umkehr data. Logan finds that at Uccle (Belgium) at 500- and 700-mbar levels, ozone increased by about 1%/yr between 1969 and 1980. Similarly, at Hohenpeissenberg (Germany) at the 500- and 700-mbar levels, ozone increased by 15% from 1967 to 1981. However, at Payerne (only 500 km away) at these same altitudes, no such trend was observed. A preliminary analysis of data from nine NH ozonesonde stations has been performed by *Liu et al.* [1980]. Eight of nine stations show ozone increases ($8 \pm 4\%$) from 1969 to 1977 in the middle troposphere, a result consistent with that reported by the *National Aeronautics and Space Administration* [1979] for the 2- to 8-km region. These ozone increases are not mirrored in surface measurements where no trends have been observed or in the southern hemisphere (SH), where one station, Aspendale, shows a decrease in tropospheric ozone 1965–1978 [*Liu et al.*, 1980]. Based on available data, one cannot distinguish a clear

lease in mineral, oil, and gas exploration and gas transmission is growing. Clearly, to be able to predict future levels of atmospheric methane, it is necessary to know the relative importance of the various methane sources and their trends. If, for example, rice agriculture is a dominant source, then trends in cultivated area, plant-strain proportions, irrigation, and multiple cropping and fertilization practices must be discerned as they affect methane release.

The dominant sink of atmospheric methane, tropospheric gaseous OH, may not be unchanging. Increased levels of tropospheric CO or of CH_4 itself can suppress OH concentrations, as has been noted by several authors. CO exhibits large hemispheric differences; these patterns and our knowledge of CO sources are reviewed by *Logan et al.* [1981]. Recently, Khalil and Rasmussen have reported evidence from measurement (in Oregon) of dramatic (6%/yr) increases of atmospheric CO between 1979 and 1983. On the other hand, W. Seiler (private communication, 1984) has measured little or no change ($\leq 1\%$/yr) in CO at several stations in both hemispheres. For a clean, background troposphere a CO increase of $x\%$ leads to a depletion of tropospheric OH of $x/(4 \pm 1)\%$, depending on altitude and various model assumptions, according to A. M. Thompson and R. J. Cicerone (unpublished manuscript, 1984). Combining the (1) source analysis by *Logan et al.* [1981], (2) information on trends of these sources (e.g., fossil fuel usage, oxidation of anthropogenic hydrocarbons), and (3) the CO data mentioned above, it is clearly possible that CO will increase by 1–2%/yr through 2030 A.D. Such an increase could cause CH_4 concentrations to increase faster (through OH suppression) than if only CH_4 source increases were considered. Because of the spectral locations of the absorption of CO, the CO increase itself is not of interest here. Its effects on the atmospheric levels of OH, CH_4, and O_3 could be very important.

Lacking all the detailed information necessary to understand the presently documented rate of increase of atmospheric CH_4 concentrations and to predict the future, we estimate that CH_4 will increase by 0.75%/yr between now and 2030; this would lead to a globally averaged CH_4 concentration of 2.34 ppm in 2030. Rates of increase of 1.5% and 0.25%/yr would lead to 3.30 and 1.85 ppm in 2030, respectively, as listed in Table 1*a*. Beyond the year 2030, when the release of continental-slope sediment methane clathrates might occur due to oceanic warming [*Revelle*, 1983], faster methane increases are possible.

2.8. *Nomethane Hydrocarbons*

In this category we include alkanes, alkenes, alkynes, aldehydes, ketones, and H_2. We pay little attention to simple aromatic compounds. By contrast with the situation for methane, there is too little information available on the concentrations, distributions, and sources of these compounds (except for C_2H_2 and H_2) to justify projections of future concentrations. For acetylene (C_2H_2), fossil fuel burning (e.g., internal combustion engines, oil-fired heaters) is a known source; its atmospheric residence time is about 4 months, and no significant biological sources are known yet [*Rudolph and Ehhalt*, 1981]. If its sources are wholly anthropogenic, an annual increase of 1–2% would be a reasonable guess. For ethane (C_2H_6), ethylene (C_2H_4), propane (C_3H_8), and propene (C_3H_6) the existing atmospheric and oceanic surface water data suggest that there are natural as well as anthropogenic sources [see, e.g., *Rudolph and Ehhalt*, 1981, and references therein]. Fugitive emissions from oil and gas wells and transmission lines are likely, of course. The state of our measurement data base for higher hydrocarbons, aldehydes (present as oxidation products of hydrocarbons), and acetone is discussed by *Penkett* [1982].

2.9. *Sulfur Compounds*

Carbonyl sulfide (OCS) is the most abundant gaseous sulfur carrier in the atmosphere. It is nearly uniformly distributed with a measured average concentration of 0.52 ppb. *Turco et al.* [1980] have examined the sources and sinks of OCS. While there are many remaining questions, they propose that up to 50% of the total source is anthropogenic. If so, OCS concentration could increase in the future, but our present understanding of OCS sinks and its atmospheric residence time is not very complete. No measured trend in OCS concentration is available at this time. Considering the lack of such data and the uncertainties about OCS sources and sinks, we cannot project other than a constant OCS abundance in Table 1*a*.

Sulfur dioxide (SO_2) is a notorious atmospheric constituent because of its role in acid deposition. In continental boundary layers where its principal source is combustion of S-containing fuels, its concentrations are often 10 ppb. Above the boundary layer its concentration is of order 100 ppt [*Maroulis et al.*, 1980]; its presence there is probably due to escape from the boundary layer below, and to oxidation of other species, e.g., OCS, CS_2, and CH_3SCH_3. Similar concentrations have been measured in the marine boundary layer [*Herrmann and Jaeschke*, 1984]. Near major anthropogenic SO_2 sources its atmospheric residence time is about 1 day (due largely to gas-to-particle conversion); in the higher troposphere in clear air its residence time is up to 1 week. Because of its very short lifetime and the uncertain future of SO_2 emission, it is not at all clear that SO_2 concentration will increase in the future. Dimethyl sulfide (DMS) is now known to exist in the oceanic boundary layer; it appears to have microbial sources in oceans that provide a significant DMS flux to the marine atmosphere [*Andreae and Raemdonck*, 1983]. Because this natural source appears to be the major DMS source and because of the short (~ 2 days) atmospheric residence time of DMS, we project no growth in its atmospheric concentrations.

Carbon disulfide (CS_2) is known to be present in background surface air at concentrations that vary from 0.03 to 0.08 ppb. However, it is virtually undetectable in the free troposphere. Excited-state oxidation [*Wine et al.*, 1981] can be an important removal process. Oceans may be a major source. No growth projection in CS_2 concentrations can be proposed reliably at this time.

2.10. *Brominated and Iodated Species*

Only a handful of species in this class have been measured in the nonurban atmosphere. The species of interest are brominated and iodated methane- and ethane-series molecules: methyl bromide (CH_3Br), methylene bromide (CH_2Br_2), bromoform ($CHBr_3$), bromotrifluoromethane or (F13B1, $CBrF_3$), methyl iodide (CH_3I), and dibromoethane ($C_2H_4Br_2$, or ethylenedibromide, EDB). CH_3Br is apparently a natural species [*Lovelock*, 1975; *Singh et al.*, 1983*b*]. Man-made emissions have the potential to perturb its global background, but only slightly. Methyl iodide is essentially all natural and, given its concentration, is predicted to remain unchanged. $CHBr_3$ and CH_2Br_2 have been measured only recently [*Berg et al.*, 1984], and too little is known about their sources to permit reasonable future projections. $CBrF_3$ (F13B1) and ethylene dibromide are exclusively anthropogenic. A continued shift toward nonleaded gasoline could offset growth that may occur in fu-

migation applications of ethylene dibromide. Because of its high carcinogenic potential, a rapid growth is not likely to be permitted in any case. $CBrF_3$ (used as a fire extinguisher) is the only brominated organic whose sink is primarily in the stratosphere (where bromine atoms can be efficient ozone destroyers). Despite its very low present abundance it can become an important carrier of organic bromine within the next 50 years. Inorganic species such as HBr, HI, BrO, IO, and NOBr are not discussed here because they are as yet undetected in the atmosphere. Their residence times are probably 5 days or less, and future trends are difficult to predict.

3. Preindustrial Era Concentrations of Greenhouse Gases

It is important to ask if CO_2 and the other trace gases should already have caused a global warming. It is very difficult, if not impossible, to answer this question for at least two reasons: (1) there are no direct data on the trace gases of interest from, say, the 1850–1940 time period, and (2) there should be a significant time lag between any increased atmospheric radiative forcing and increased global temperatures, due to oceanic heat capacity. To allow at least a rough estimate of the size of the effect due to increased trace gas concentrations from about 1880 until 1980, we will attempt to estimate the 1880 concentrations of methane, nitrous oxide, chlorofluorocarbons, CCl_4, and tropospheric ozone. The proposed preindustrial concentrations of the trace gases are shown in Table 1*b*.

For CO_2, the *National Research Council* [1983] study suggests that the most likely preindustrial value is between 260 and 290 ppm. For this study, the preindustrial concentration of CO_2 is assumed to be 275 ppm.

For CH_4, the data of *Craig and Chou* [1982] show that CH_4 has increased monotonically for the past 400 years; these data are CH_4 concentrations in air trapped in dated Greenland ice cores. Craig and Chou noted that there is as much as a 90 year uncertainty in the age of this air, depending on whether air moved freely throught the firn phase of the snow above the firn-closure depth. If the air at the 90-year firn level was zero years old, then the CH_4 concentration in the year 1880 was about 1.05 ppm. If the air there was not so young, the Craig and Chou data show that the CH_4 concentration in 1880 had to be over 1.05 ppm. If, for example, the air in 90-year old ice at this site were 50 years old instead of zero years old, the implied 1880 CH_4 concentration would be 1.10–1.15 ppm in 1880. We assume that the 1880 CH_4 level was 1.15 ppm.

For nitrous oxide, there are no direct data from pre-1900; indeed, N_2O was discovered in the atmosphere only in 1938. Modern data from 1976–1980 and from 1961–1974 have been used by *Weiss* [1981] to estimate a preindustrial atmosphere N_2O concentration of 281–291 ppb. Accordingly, we assign a value of 285 ppb to N_2O for the year 1880.

The chlorofluorocarbons and fluorocarbons (CCl_2F_2, CCl_3F, and the other compounds listed in Table 1 are almost certainly of exclusive and post-1940 anthropogenic origin [*National Academy of Sciences/National Research Council*, 1979]. Therefore we estimate that each of them was absent from the 1880 atmosphere.

Carbontetrachloride is more interesting. It is known to be produced by marine organisms [see, e.g., *Fenical*, 1982], yet its mid-1970's (and present) concentration can be explained by anthropogenic emissions [*Singh et al.*, 1976]. Because of the apparent unimportance of current natural sources, we will assume that it was essentially absent from the 1880 atmosphere.

Of the important greenhouse gases, tropospheric ozone is most difficult for which to estimate differences between present-day concentrations and those of one century ago. The surplus of NH over SH ozone, the more pronounced seasonal cycle in the NH ozone data, the strong theoretical case for excess ozone production in the industrialized NH and the hints of a positive trend since 1967, all imply that there was less O_3 in the 1880 NH troposphere. Detailed examination of these and other factors [see *Levy et al.*, 1985] does not allow one to state with confidence that the hemispheric or global background tropospheric ozone is strongly controlled by photochemical reactions (such as those between hydrocarbons and nitrogen oxides to produce ozone). For example, there is evidence that the NH troposphere receives perhaps 3 times as much ozone from the stratosphere as does the SH troposphere. One would predict higher NH concentrations from this meteorological input of ozone, although the higher surface-destruction rates in the NH would offset some of the additional input. Perhaps 50% more ozone is observed in the NH tropics than in the SH tropics (0- to 12-km altitude; *Fishman et al.* [1979*b*]) and 25–50% more in the midlatitudes of the NH at 800-mbar pressure levels than at corresponding SH locations. Another feature of ozone in the NH midtroposphere, the east-west gradient over North America [*Chatfield and Harrison*, 1977], appears to be evidence for photochemical production over continents. We assume that half of the difference between NH and SH is due to anthropogenic emissions (and that 1880 emission of NO_x and hydrocarbons was negligible compared with those in 1980). Even with these assumptions, one is left with uncertainty about vertical profiles. In the upper troposphere, there is more influence from the stratosphere, but there is also significant existing potential for human impact by direct injections from aircraft [*Liu et al.*, 1980]. As a very rough estimate, we will guess that there was 25% less ozone in the 1880 NH troposphere than in 1980 NH troposphere and that SH tropospheric ozone did not change during that century.

4. Description of the Climate Model

The direct radiative effects of trace gases are included in this study. The effects due to altered chemistry are included explicitly as far as stratospheric O_3 perturbation is considered and implicitly with respect to tropospheric O_3, i.e., projected O_3 increases can be considered to arise from the projected increases in hydrocarbons, CO, and NO. With respect to the feedback effects, this study accounts for troposphere/stratosphere radiative interactions and the feedback between temperature and chemistry within the stratosphere. The climate-chemistry interactions in the troposphere and the possible effects of temperature changes on stratospheric H_2O are ignored. Both of these feedback effects, while they may be relatively smaller than the direct radiative effects would require coupled photochemical climate models [*Callis et al.*, 1983].

A brief description follows of the radiative-convective model and the source for the spectroscopic data used for the computations.

4.1. *Radiative-Convective Model*

The one-dimensional radiative-convective model described by *Ramanathan* [1981] is adopted. This model, hereafter referred to as model R, has a surface boundary layer which

explicitly allows for the surface-atmosphere exchange of latent and sensible heat and also solves for the boundary layer moisture [*Ramanathan*, 1981, equations 17–20, Figure 7]. The standard radiative-convective models [e.g., *Manabe and Wetherald*, 1967; *Ramanathan and Coakley*, 1978] ignore these processes and do not treat explicitly the exchange of latent heat flux between the surface and the free atmosphere.

The boundary layer moisture and hence the relative humidity are explicitly computed in the model, but the tropospheric relative humidity is prescribed as discussed by *Ramanathan* [1981]. The mass mixing ratio of H_2O above 12 km is prescribed to be 2.5 ppm. Because of the explicit treatment of the boundary layer, the model R computes the surface temperature and the surface air temperature. Standard radiative-convective models compute only one temperature for the lower boundary which can be interpreted as an average of the surface and surface air temperature. In model R the surface air temperature change is larger than that of the surface temperature change by about 10–13%. This point should be noted when comparing the present calculations with the published results.

4.2. *Radiation Model and Spectroscopic Data*

The trace gases, their longwave band centers, and the adopted band strengths are shown in Table 4. The treatment of H_2O, O_3, CO_2, and CH_4 are as described in model R. For CO_2, one of us (J.T.K.) incorporated the more detailed band model of *Kiehl and Ramanathan* [1983] in model R. The surface warming due to doubled CO_2 estimated with the detailed CO_2 scheme was in excellent agreement (within 5%) with that estimated from the somewhat simpler scheme in model R. For CH_4, model R employs the *Donner and Ramanathan* [1980] band model. Although the band strength adopted in model R is stronger than the current accepted value by about 35%, the band model parameters were fit to give agreement with laboratory absorptances. Hence the CH_4 radiative forcing estimated by this band model agrees within 5–10% of that estimated from a 5 cm^{-1} spectral resolution narrow band model which employs recent [*Rothman et al.*, 1983] line data. Numerous modifications were incorporated in model R to treat the effects of the minor trace gases included in this study and these modifications are described below.

N_2O. The R scheme used the *Donner and Ramanathan* [1980] band model scheme. We have retained this scheme, but included the following N_2O bands that were ignored by *Donner and Ramanathan* [1980]: the two-band systems centered at 1168 cm^{-1}, one of which is the $2\nu_4$ band of the four isotopes with bandstrength 8.5 cm^{-1} (cm atm)$^{-1}$ STP and the hot bands of the four isotopes with band strength 1.5 cm^{-1} (cm atm^{-1}) STP. Although these bands are considerably weaker than the fundamental ν_1 band system centered at 1285 cm^{-1}, they contribute as much as 20% of the ν_1 band system to the surface warming due to N_2O. This disproportionately large contribution by the weak bands arises because N_2O is almost in the strong line limit, and hence the opacity scales as the square root of the band strength. Hence for gases whose concentration are large and their band strengths are sufficiently strong that they are in the strong line limit, great care must be exercised in including all the bands whose strengths are smaller by as much as 2 orders of magnitude than the strong fundamental band. This is the reason why the present model incorporates many isotopic and hot bands of trace gases such as CO_2, N_2O, and CH_4.

Other trace gases. The band absorption A is expressed as

$$A = \Delta\omega\left[1 - \sum_{i=1}^{N} f_i e^{-\tau_i/\bar{\mu}}\right] \tag{1}$$

$$\tau_i = \left(\frac{k_i}{f_i}\right)\left(\frac{Sw}{\Delta\omega}\right) \tag{2}$$

$$\sum_{i=1}^{N} f_i = 1 \tag{3}$$

$$\sum_{i=1}^{N} k_i = 1 \tag{4}$$

where $\Delta\omega$ is the band width in cm^{-1}, S is the band strength in cm^{-1} (cm atm)$^{-1}$, w is the absorber amount in cm atm. The above procedure of expressing the band transmission as a sum of transmission functions averaged over pseudo-spectral intervals i with weighting functions f_i and k_i is essentially the exponential-sum fitting method described by *Wiscombe and Evans* [1977]. The procedure of employing $\bar{\mu}$ to approximate the solid angle integration of the transmission is referred to as the exponential kernel approximation [*Sparrow and Cess*, 1970, p. 226]. However, instead of adopting the standard procedure of employing one value for $\bar{\mu}$, we obtain exact values of $\bar{\mu}$ as a function of the optical depth from tabulated values of the E_3 exponential kernel function [see *Sparrow and Cess*, 1970, pp. 200, 312]. The values of $\bar{\mu}$ as a function of τ is fit by the following smooth expression:

$$(\bar{\mu})^{-1} = 1.5 + \frac{0.5}{1 + 4\tau + 10\tau^2}\,. \tag{5}$$

In (5), the optical depth τ is the total optical depth, i.e., the sum of the optical depths of all gases in the interval. The above set of equations is mathematically and conceptually rigorous if one of the two following asymptotic limits are satisfied.

1. The optically thin limit, i.e., $\tau_i \ll 1$. In this limit, (1)–(5) reduce to

$$A = 2Sw \tag{6}$$

It can be easily shown that (6) is the exact expression for the band absorption in the optically thin limit. *Ramanathan* [1975] used this expression to treat the $CFCl_3$ and CF_2Cl_2 bands.

2. The smeared out line structure limit. In this limit, the line spacing between neighboring lines is much smaller when compared with the line half-width. Consequently, the lines are smeared out and the absorption coefficient follows a smooth variation with wavelength. This limit is adequately satisfied for the $CFCl_3$ and CF_2Cl_2 bands, as can be inferred from the

TABLE 3. Band Parameters for Trace Gases that Employ Equation (1) for the Band Absorption

Species	$\Delta\omega$, cm^{-1}	N	i	f_i	k_i
$CFCl_3$ (CFC11)	60	3	1	0.25	0.72
			2	0.25	0.22
			3	0.5	0.06
CF_2Cl_2 (CFC12)	60	2	1	0.25	0.52
			2	0.75	0.48
CF_4	20	1	1	1	1
All others	60	1	1	1	1

TABLE 4. Band Locations and Strengths

Trace Gas	Band Center, cm^{-1}	Band Strengths, cm^{-1} (atm cm)$^{-1}$ STP: Range of Measurements	Band Strengths, cm^{-1} (atm cm)$^{-1}$ STP: Value Adopted[2]	Reference[1]
CO_2	667	[3]	44 bands incl.	M
N_2O	589	20.7–40.3	27(F, 1H, 4I)	M
	1168	8.5–12	10(F, 1H, 4I)[4]	
	1285	242–384	234.5(F, 1H, 4I)	
CF_4 (F14)	632	42–62	54.7	P
	1261($2\nu_4$)	4175–5934	4175	
	1285(ν_3)			
C_2F_6 (F116)	714		146	P
	1116		1057	
	1250		3658	
CF_3Cl (F13)	783		157	P
	1102		2505	
	1210		3000	
CF_2Cl_2 (F12)	915	1370–1568	1567.5	K
	1095	1237–1330	1236.8	
	1152	789–893	835.8	
$CHClF_2$ (F22)	810		237	N
	1110		691	
	1310		109	
$CFCl_3$ (F11)	846	1670–1965	1965	K
	1085	576–781	736	
CH_2Cl_2	717	35	35	P
	758	424–548	424	
	898	4.3–5.4	5.4	
	1268	119–147	118.7	
$CHCl_3$	774	864–1201	1009	P
	1220	140–206	140	
CCl_4	776	1317–2026	1437	P
CH_3CCl_3	725		299.8	N
	1080		167	
	1385		14.2	
CH_4	1306	148–185	185	P
	1534	2–3		P
C_2H_2	730	724–804	801	P
	1328	95.6–101.1	95.6	P
SO_2	518	116–125		P
	1151	96–106.8	106.8	
	1362	844–857	857	
Ozone	1041	356–382	376	M
	1103	10–11	11	
	590		78	
	790		321	N
PAN	1160		326	
	1300		272	
	1730		576	
CHF_3	1117–1152		3838.5	P
CH_2F_2	1090		1314	P
$CBrF_3$	1085		2069.3	P
	1209		2074.7	

[1]The reference is for the value adopted in this study: M, *McClatchey et al.* [1973]; N, H. Niki (personal communication, 1983); P, *Pugh and Rao* [1976]; and K, *Kagann et al.* [1983].

[2]F, fundamental band; 1H, first hot band; I, isotopic band. 4I denotes four isotopic bands.

[3]Minimum of 44 isotopic, fundamental, and hot bands are required.

[4]Treated as two band systems: one for the $2\nu_4$ band and one for the hot band, and each system has four isotope bands.

line parameters given by *Goldman et al.* [1976a]. Inspection of published spectra reveals that this limit is more than adequately satisfied for most other polyatomic trace gases considered here.

The values of the band parameters and band strengths are given in Tables 3 and 4, respectively. In order to examine the validity of the present approach (i.e., (1)), we computed the surface-troposphere heating due to the strongest band of $CFCl_3$ (F11) with a fine spectral resolution model which computes transmittances at 1 cm^{-1} intervals employing line parameters given by *Goldman et al.* [1976a] and performs angular integration with a 12-point Gaussian quadrature scheme. As shown in the next section, the surface-troposphere heating estimated by employing (1) agrees within 4% with that obtained from the detailed computations. The procedure adopted in the present study for the various trace gases is summarized below.

1. For all trace gases except H_2O, CO_2, CH_4, N_2O, and O_3, (1)–(5) are adopted.
2. The parameter, $\Delta\omega$, is assumed to be 60 cm^{-1} for all of

the bands, except CF_4, for which $\Delta\omega = 20\ cm^{-1}$. These values are chosen by inspection of the published spectra. For example, *Goldman et al.* [1976a, b] have shown the spectra for the strongest bands of $CFCl_3$ and CF_2Cl_2. For the $CFCl_3$ band at 846 cm^{-1}, the line strengths in the band wings around 810 and 869 cm^{-1} are smaller by 2 orders of magnitude than their values near the band center. For the CF_2Cl_2 band, the $\Delta\omega$ can be as large as 100 cm^{-1}, but our calculations are rather insensitive to $\Delta\omega$ for $\Delta\omega > 40\ cm^{-1}$. The CF_4 band at 1285 cm^{-1} appears to be extremely narrow [*Goldman et al.*, 1979]. Although we have chosen 20 cm^{-1}, we have examined values as low as 5 cm^{-1}, and these results will be discussed subsequently.

3. For $CFCl_3$ and CF_2Cl_2, the exponential-sum fit parameters N, f_i, and k_i are obtained from the random model line parameters published by *Goldman et al.* [1976a, b]. Note however, as mentioned later, the band strengths are obtained from *Kagann et al.* [1983]. For all other gases, the relevant line parameters are not available, and hence we let $N = 1$. This in turn forces $k_i = 1$ and $f_i = 1$ because of the consistency relationship expressed in (3) and (4).

4. We employ an accurate procedure for evaluating the Planck function. For $\omega > 1000\ cm^{-1}$, the Planck variation with ω is so strong that, the Planck function evaluated at the band center (a commonly adopted procedure in climate models) can differ from the mean value for the band by as much as 10–15%. To avoid such errors, the Planck function is evaluated at 10 cm^{-1} intervals within the band, and a mean value for the band is obtained by averaging the narrow band values.

5. Band strengths: Except for $CFCl_3$, CF_2Cl_2, CH_3CCl_3, CFC22, and PAN, we have relied heavily on the published summary by *Pugh and Rao* [1976], denoted as P in Table 4. These authors give a range of measured values, which are reproduced in Table 4. For this study, we have chosen the values measured after the 1970's, and if these were not available, we adopted the middle value of the range given in P. For $CFCl_3$ and CF_2Cl_2 we have adopted the most recent values of *Kagann et al.* [1983]. For the CF_4 ν_3 band at 1285 cm^{-1}, *Wang et al.* [1980] have employed a value of 5934 cm^{-1} (cm atm)$^{-1}$ based on *Saeki et al.*'s [1976] measurements. This value is beyond the range given by *Pugh and Rao* [1976], and furthermore, the recent measurements by *Goldman et al.* [1979] yield a value of 4500 cm^{-2} atm^{-1}. The band strengths for CH_3CCl_3, $CHClF_2$ (F22), and PAN are not available in the open literature. High-resolution spectral data for these bands and integrated band strengths were kindly supplied to us by H. Niki (personal communication, 1983), whose values are shown in Table 4 as N.

6. The CFC's and other trace gases besides CO_2 are assumed to be mixed uniformly from the surface up to 12 km, above which the mixing ratio is assumed to decrease with a scale height of 3 km. However, as shown by *Fabian et al.* [1984], the mixing ratios of long-lived species such as CF_4, C_2F_6, and CF_3Cl are nearly constant from the surface to the middle stratosphere (~30 km). In the next section we will examine the sensitivity of the greenhouse effect to the mixing-ratio profile. CH_4, N_2O, and CO_2 are assumed to be uniformly mixed throughout the atmosphere. The observed mixing ratio of CH_4 and N_2O decreases with height above 12 km. However, as shown in the next section, the computed surface warming due to CH_4 and N_2O increase is insensitive to their mixing-ratio profile in the stratosphere. The O_3 profile is taken from the hemispherical, annual data given by *Ramanathan and Dickinson* [1979].

7. We have allowed for the overlap of all of the minor trace gas bands with H_2O, CO_2, O_3, CH_4, N_2O, and CFC's and the mutual overlap of these gases. In certain spectral locations, e.g., 1285 cm^{-1}, as many as four gases have strong overlapping bands, and such effects are included in the calculations. For all of the trace gases with band centers shortward of 8 μm and longwave of 12 μm, the overlap with CH_4, N_2O, CO_2, or H_2O is treated by adopting the Malkmus narrow-band model. The transmission is computed with a spectral resolution of 20 cm^{-1}. The line parameters are derived from the 1982 Air Force Geophysics Laboratory (AFGL) line tape [*Rothman et al.*, 1983]. Hence the overlap treatment does not follow the broadband model approach.

In summary, the number of trace gases included in this study, together with the treatment of the overlap between the various gases and the details of the various fundamental, hot, and isotopic bands, make the present study the most comprehensive climate model calculations that have been performed so far for the trace gas climate effects.

4.3. *Accuracy of the Trace Gas Radiative Treatment*

The accuracy of the treatment as given by (1)–(5) is examined by performing detailed narrow-band calculations for the $CFCl_3$ band at 11.8 μm. This band is chosen because it is the strongest of the CFC bands and hence provides a stringent test of the present scheme. Furthermore, random-band model parameters, with a spectral resolution of 1 cm^{-1}, for this band have been provided by *Goldman et al.* [1976a]. For the reference calculations, a Malkmus random-band model with a spectral resolution of 1 cm^{-1} is employed. The details of this model are given by *Kiehl and Ramanathan* [1983]. The angular integration within each spectral interval is performed with a 12-point Gaussian quadrature. The model atmosphere represents midlatitude summer condition with no clouds. In Table 5, the change in the net (down-up) flux at the tropopause, i.e., the surface-troposphere heating, due to increase of CFC11 from 0 to 2 ppb as computed by the reference model is compared with that obtained from the present scheme, i.e., (1)–(5). Also shown in this table, for comparison purposes, is the result obtained from (6), which is the form of the optically thin limit equation employed by *Ramanathan* [1975]. It is seen that the present scheme is in excellent agreement with the more detailed calculations. The equation for the optically thin assumption employed by *Ramanathan* [1975] overestimates the heating by about 16%. However as shown later, the sur-

TABLE 5. Surface-Troposphere Heating due to CFC11 846-cm^{-1} Band

Model*	F, W m^{-2}	Comment
Reference	0.51	Narrow-band model with 1-cm^{-1} resolution; 12-point Gauss quadrature for angular integration.
Present scheme	0.525	Equations (1)–(5). Parameters from Table 3.
Optically thin approximation	0.59	Equation (6)

Atmosphere: midlatitude clear-sky conditions. F: surface-troposphere heating due to increase of CFC11 from 0 to 2 ppb.

*For comparison purposes, all the three models adopt the spectroscopic parameters from *Goldman et al.* [1976a].

TABLE 6. Examples of the Effect of Overlapping of Absorption Bands on the Computed Surface Warming

Constituent	Change	With Overlap*		Without Overlap
		ΔT_s	ΔT_g	ΔT_g
CH_4†	1.25X	0.09	0.08	0.19
N_2O†	1.25X	0.12	0.1	0.2
CF_2Cl_2 (F12)‡	0–1 ppb	0.16	0.15	0.19
$CFCl_3$ (F11)	0–1 ppb	0.14	0.13	0.16
CF_4 (F14)	0–1 ppb	≈0.06	≈0.05	0.12
CF_3Cl (F13)	0–1 ppb	0.22	0.2	0.25
CH_2Cl_2	0–1 ppb	≈0.03	≈0.02	0.04
$CHCl_3$	0–1 ppb	≈0.06	≈0.06	0.09
CCl_4	0–1 ppb	≈0.08	≈0.07	0.11
C_2H_2	0–1 ppb	≈0.02	≈0.02	0.07
C_2F_6 (F116)	0–1 ppb	0.13	0.12	0.2
CH_3CCl_3	0–1 ppb	≈0.02	≈0.01	0.04
PAN	0–1 ppb	≈0.04	≈0.03	0.06

ΔT_s is surface-air temperature change, and ΔT_g is surface (or ground) temperature change.

*Numbers have been rounded off; when ΔT is less than about 0.02 K, because of the convergence criterion, the result may be uncertain by as much as ±30%.

†CH_4 and N_2O are assumed to be uniformly mixed from the surface to the top of the atmosphere. However, these calculations, when repeated with observed profiles which show a decrease in the mixing ratio above 12 km, yield ΔT results identical to those shown in this table.

‡For this gas and for all the others following it, the mixing ratio decreases above 12 km with a scale height of 3 km. The computed surface warming is larger by about 15% when the mixing ratio above 12 km is held constant at the surface value.

face warming due to increase of CFC's computed with the present accurate scheme is in excellent agreement with that estimated by *Ramanathan* [1975]. The agreement is because of the following compensating effects: (1) the band strengths used in *Ramanathan* [1975] are smaller by about 10% than the recent values used in this study; (2) the 16% error shown in Table 5 is reduced somewhat with the inclusion of clouds; (3) the error in the optically thin approximation is smaller for the other bands of CFC11 and 12 whose strengths are considerably smaller than the 11.8-μm CFC11 band.

Cess [1982] has also performed similar narrow-band calculations for $CFCl_3$ and showed that the smeared-out line structure assumption, which is invoked in arriving at (1), is an excellent approximation for CFC bands. In summary, we conclude that the present scheme is very accurate. The only source of remaining error is the neglect of the temperature dependence of the hot bands of CFC's that have been detected, in the vicinity of the strong $CFCl_3$ and CF_2Cl_2 bands, by *Varanasi and Ko* [1977] and *Nanes et al.* [1980]. While the effects of the hot bands are included in this study, the temperature dependence of their band strengths arising from the temperature dependence of the excited vibrational states is ignored. *Nanes et al.* [1980], however, suggest only a weak temperature dependence. As a note of caution, we add that the temperature dependence mentioned above should not be confused with the temperature correction that is needed to convert band strengths, S, measured at temperature T to STP conditions. Recall that in (1), the path length w is in cm atm, STP, and hence S measured at a temperature T in the units of cm^{-1} (cm atm)$^{-1}$ should be multiplied by $(T/273)$ to convert to the units of cm^{-1} (cm atm)$^{-1}$, STP. In some instances in the literature, this correction factor has been confused for the temperature dependence of S. The procedure of employing the correction factor $(T/273)$ is rigorous for the fundamental CFC bands. For the hot bands, however, we need an additional term to account for the temperature dependence of the excited vibrational state [e.g., see *Kiehl and Ramanathan*, 1983, equation 12].

5. RESULTS

5.1. *Uniform Increase in Certain Trace Gases*

Before presenting the results for the trace gas scenario shown in Table 1*a*, we will discuss results for a hypothetical case of 0–1 ppb increase for several of the trace gases. The purpose of this exercise is twofold: to elucidate the processes that determine the magnitude of the trace gas effects and to identify the most important trace gases from a climate viewpoint. For these two objectives, we avoid specific scenarios to assure that conclusions are not scenario dependent.

The computed surface warming due to a 0–1 ppb increase in 15 different trace gases is shown in Figure 1. The tropospheric O_3, CH_4, and N_2O effects are relatively better known and are shown merely for comparison purposes. Several interesting and rather surprising features of the results shown in Figure 1 are noted below.

TABLE 7. Computed Surface Temperature Change Resulting From Increasing CFC's From 0 to 2 ppbv[1]

Item	Model	FCA,[2] K	FCT,[3] K	Empirical,[4] K
1	*Ramanathan* [1975]	0.56[5]	0.9	0.9
2	*Reck and Fry* [1978]	0.76[6]		
3	*Chamberlain et al.* [1982]			1.42
4	*Wang et al.* [1976]	0.38	0.56	
5	*Wang et al.* [1980]		0.69	
6	*Hansen et al.* [1982]		0.50	
7	*Lacis et al.* [1981]		0.65	
8	*Karol et al.* [1981]	0.8		
9	*Hummel and Reck* [1981]	0.76		
10	This study[7]	0.55–0.6[8]		
11	This study (uniformly mixed)[9]	0.63–0.7[8]		
12	This study: CFC band strengths from *Ramanathan* [1975]	0.51–0.56[8]		
13	This study: CFC band strengths from *Varanasi and Ko* [1977]	0.50–0.55[8]		

Comparison of various model results. $CFCl_3$ and CF_2Cl_2 are each increased from 0 to 2 ppbv.

[1]*Ramanathan* [1975], this study, and the GISS models (items 4–6) assume a constant CFC mixing ratio from the ground to 12 km, and above 12 km the mixing ratio decreases exponentially with a scale height of 3 km. *Reck and Fry* [1978], *Karol et al.* [1981], and *Hummel and Reck* [1981] assume a constant CFC mixing ratio from the ground to the top of the atmosphere.

[2]One-dimensional radiative-convective model with fixed relative humidity and with fixed-cloud altitude (FCA).

[3]Same as footnote 2, but with fixed-cloud temperature (FCT) instead of fixed-cloud altitude.

[4]Estimated from an empirical expression for the surface temperature sensitivity parameter.

[5]The FCA model results were not mentioned by *Ramanathan* [1975] but were obtained for the purposes of the present comparison.

[6]Reck and Fry gave ΔT results for 1-ppbv increase, which was linearly scaled for the 2-ppbv increase.

[7]CFC mixing ratio as described by *Ramanathan* [1975]. See footnote 1 above.

[8]The lower value is surface temperature change, and upper value is surface air temperature change.

[9]CFC mixing ratio is constant from surface to top of the atmosphere.

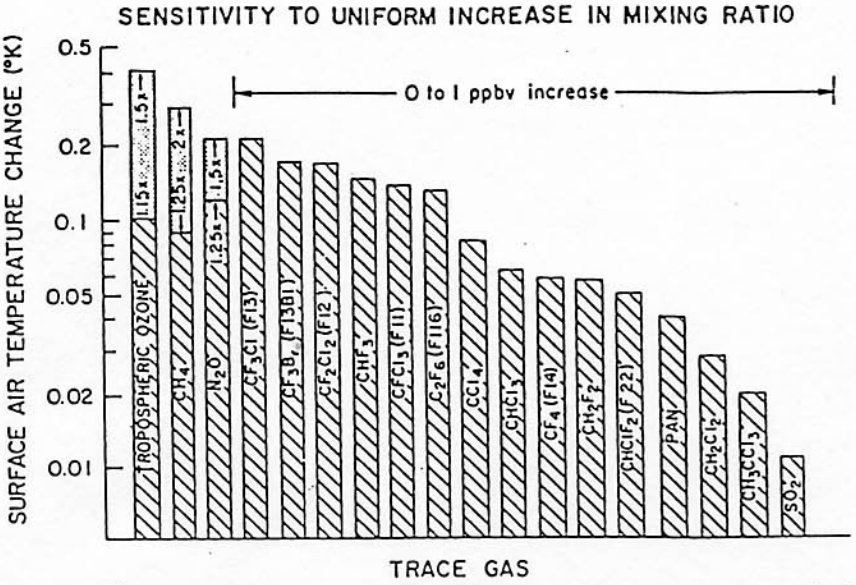

Fig. 1. Surface temperature increase due to a 0–1 ppbv increase in trace gas concentration. Tropospheric O_3, CH_4, and N_2O increases are also shown for comparison.

1. Among the other trace gases, $CFCl_3$, CF_2Cl_2, CF_3Cl, C_2F_6, CHF_3, and $CBrF_3$ exert the largest surface warming effect. The contribution by CF_3Cl, C_2F_6, CHF_3, and $CBrF_3$ has not been discussed before and is a surprising and new aspect of the present results. The primary reason is the strength of their bands, and as shown in Table 4, the strongest bands of these gases are stronger than the strongest bands of $CFCl_3$ and CF_2Cl_2 by more than a factor of 2. The location of the band center, however, plays a crucial role because of the overlap effect. For example, in the 1295-cm^{-1} region, the absorption by N_2O, CH_4, and H_2O bands saturates this region, and hence trace gases in this spectral region have relatively lesser impact on climate. This is the primary reason why CF_4, although possessing a band in the 1285-cm^{-1} region which is stronger than any other bands in the 8- to 20-μm region, produces a surface warming of only 0.06 K.

2. The sensitivity of surface temperature to tropospheric ozone has been anticipated earlier [*Ramanathan and Dickinson*, 1979] but has not received much consideration elsewhere in the literature.

3. Although PAN has several moderately strong bands, its strongest band is in the middle of the strong 6.3-μm H_2O bands. Similarly, although CCl_4 and $CHCl_3$ have moderately strong bands, their strongest bands are located in the 774-cm^{-1} region, where they are overlapped by CO_2, H_2O rotation bands, and the H_2O continuum.

4. To illustrate the importance of the overlap problem, we show in Table 6 the surface temperature increase with and without the overlap effects. Such results, besides illustrating the contribution from various radiative processes, also facilitate model intercomparison study by enabling the identification of the sources for model differences. We also show in this table, the surface and surface air temperature change for one of the two cases. In general, surface air temperature is larger than the surface temperature change by about 10%. It is clear from Table 6 that for several trace gases, e.g., CF_4, $CHCl_3$, CH_3CCl_3, C_2F_6, the overlap effect ameliorates ΔT_s by factors of 1.5–2.

We will now compare the present estimates of ΔT_s with other published estimates for a few of the trace gases. Consider first $CFCl_3$ and CF_2Cl_2 for which the differences between the various model estimates of the global surface temperature change are disturbingly large as illustrated in Table 7. The differences shown in Table 7 can arise from differences in the radiative treatment and (or) from differences in the model sensitivity. In order to isolate these two sources, the climate sensitivity parameter, λ, as estimated from various models is shown in Table 8. As explained by *Dickinson* [1982] and *Ramanathan* [1982], λ and ΔT_s are approximately related by

$$\Delta T_s \approx \lambda \Delta F \tag{7}$$

where ΔF is the radiative forcing of the surface-troposphere system due solely to trace gas increase, i.e., CFC increase in the present example. As described below, Tables 7 and 8 provide the answers for all of the differences in the computed ΔT_s.

1. There is a wide spread in the measured band strengths. For example, Figure 2 shows the measured band strengths by various investigators for the strongest CFC bands. The present study uses the recent measurements of *Kagann et al.* [1983], whereas all of the other studies employ the earlier measurements. The values used by *Ramanathan* [1975] underestimate (compare item 12 with item 10) ΔT_s by 8% while Varanasi and Ko's values employed in the Goddard Institute for Space Studies (GISS) models underestimate (compare item 13 with item 10) ΔT_s by 10%.

2. With respect to the radiative treatment, *Ramanathan* [1975] and *Chamberlain et al.* [1982] employ (6), which is one form of the optically thin approximation. By comparing item 12 with 1, both of which use the same band strengths, it is seen that (6) overestimates ΔT_s by about 5%. However, the present study which uses an accurate procedure is in excellent agreement with *Ramanathan* [1975] because of the compensating effects of the smaller band strengths used in that study. The other models cited in Table 7, unfortunately, do not give the equation or the details of their radiative treatment. However, all of these models rely primarily on integrated band strengths and hence must employ the optically thin approximation, but not necessarily (6).

3. The unrealistically large value obtained by *Chamberlain et al.* [1982] results primarily from their approach of esti-

TABLE 8. Comparison of Model Climate Sensitivity Parameter

Model	λ, K/W m^{-2}	f^a	f (empirical)
Manabe and Wetherald [1967]	0.53		
Ramanathan [1975]	0.52	1.6	1.6
Reck and Fry [1978]	0.53		
Wang et al. [1976]	0.47	1.5	
Wang et al. [1980]	0.47	1.23	
Hansen et al. [1982]	0.47	1.4	
Lacis et al. [1981]	0.47	1.4	
This study	0.52		

Here, $f^a = \lambda(\text{FCT})/\lambda(\text{FCA})$; $f(\text{empirical}) = \lambda(\text{empirical})/\lambda(\text{FCA})$. See Table 7 (footnotes 2 and 3) for explanation of FCA and FCT.

mating the CFC heating from the change in the net flux at the surface rather than at the tropopause (see *Ramanathan* [1982] for more details on this topic).

4. *Hummel and Reck* [1981], *Karol et al.* [1981], and *Reck and Fry* [1978] assume the CFC mixing ratio to be uniform from the surface to the model top, whereas *Ramanathan* [1975], the present study, and the GISS models assume an exponentially decaying mixing ratio (see footnote 1 in Table 7) in the stratosphere. Our model calculations, when repeated with a constant mixing ratio, show that the constant mixing ratio overestimates (compare items 10 and 11) ΔT_s by about 15%. Reducing these constant mixing-ratio model estimates by 15% would bring them closer to the present values.

5. This brings us to the GISS models. First note from Table 7, the estimates from the various versions of these models have undergone substantial change. We will adopt the latest result of *Lacis et al.* [1981] as their best estimate and compare this with that of the present study. Lacis et al. have not given the result for the fixed-cloud altitude (FCA) model, but using the factor $f^a(=1.4)$ in Table 8, we infer from Table 7 that the Lacis et al. result for the FCA version is 0.46 K (=0.65/1.4). The sensitivity of their model is smaller than that of the present model by 11% (=0.52/0.47). Furthermore, Varanasi and Ko's band strengths used in their study underestimates ΔT_s by 10% (compare items 10 and 13 in Table 7). Their model result of 0.46 K when corrected for the above differences increases to 0.56 (0.46 × 1.11 × 1.1), which is in close agreement with the present estimate of 0.55–0.6 K.

In summary, we can account for almost all of the differences between the various model estimates. The analyses lead to the conclusion that, in view of the accurate treatment of the CFC radiative effects and in view of the detailed and up-to-date spectroscopic information incorporated in this study, the present estimates of 0.55–0.6 K for CFC increase from 0 to 2 ppb should be considered as the state-of-the art estimates for a radiative-convective model with fixed cloud top altitude.

For CF_4, the only available calculation is that of *Wang et al.* [1980], who compute a surface temperature change, for 0–1 ppbv change in CF_4, of 0.07 K to be compared with the present value of 0.06 K. Although the close agreement is reassuring, there are substantial differences in the CF_4 treatment between the two models. Wang et al.'s band strength is larger than the present study value by 40% and also they assume a 5-cm^{-1} bandwidth. Decreasing the bandwidth from 20 to 5 cm^{-1} in the present model leads to about 20% reduction in ΔT_s, while increasing the band strength to Wang et al.'s value of 5934 cm^{-2} atm^{-1} leads to abut 25% increase in ΔT_s. It is not clear how the overlap of CF_4 with H_2O, N_2O, and CH_4 is treated in Wang et al.'s model calculations.

Hummel and Reck [1981] have computed the effects of $CHClF_2$ (CFC22), CH_3CCl_3, and CH_2Cl_2. Their surface warming for $CHClF_2$, CH_3CCL_3, and CH_2Cl_2 are, respectively, (for 0–1 ppb increase) 0.04, 0.02, and 0.01, and the respective results of the present study are 0.05, 0.02, and 0.01 K. The two models seem to be in good agreement. Since *Hummel and Reck* [1981] have given neither the quantitative details of their radiation model nor the band strengths, it is difficult to rule out the possibility of a fortuitous agreement.

Sensitivity to vertical distribution. The sensitivity of the computed surface temperature change to vertical O_3 distribution is discussed in the next section. The discussion here is restricted to those gases that are uniformly mixed in the troposphere, i.e., all of the gases, other than O_3, shown in Figure 1.

Observed profiles of CH_4 and N_2O reveal a decrease in the mixing ratio above about 12 km as opposed to the constant mixing-ratio profile assumed in this study. The scale height for the mixing ratio depends strongly on latitude [*World Meteorological Organization*, 1982*b*]. Midlatitude profiles show a sharper decrease (scale height ≈8 km) with altitude than tropical profiles (scale height >15 km). We repeated the surface temperature calculations with the observed midlatitude profiles [*World Meteorological Organization*, 1982*b*, Figures 1-43 and 1-44]. For a doubling of CH_4, both the uniform mixing-ratio profile and the midlatitude profile yielded a ΔT_s of 0.31 K. Similarly, for a doubling of N_2O, both mixing ratio profiles yielded a ΔT_s of 0.4 K. The scale height of the mixing ratio for CH_4 and N_2O is sufficiently large (≥8 km) that the stratospheric column abundance (of CH_4 and N_2O) for the uniform mixing-ratio profile and the observed profile is nearly the same, and hence both profiles yield the same surface warming.

For all of the other trace gases shown in Figure 1, the computed ΔT_s is about 15% larger for the uniform mixing-ratio profile than for the reference profile (assumed in this study) in which the mixing ratio decreases (above 12 km) with

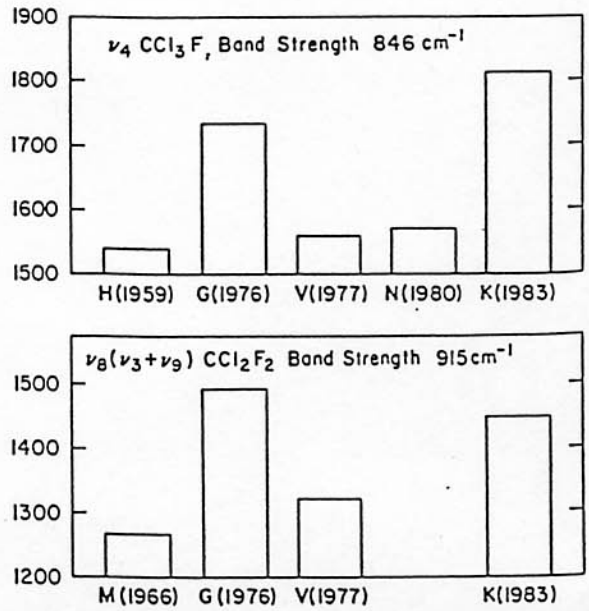

Fig. 2. Band strengths for the ν_4 CCl_2F_2 bands in units of cm^{-2} atm^{-1} at 296°K. Sources for band strengths are H(1959), *Herranz et al.* [1959]; G(1976), *Goldman et al.* [1976*a*, *b*]; V(1977), *Varanasi and Ko* [1977]; N(1980), *Nanes et al.* [1980]; and K(1983), *Kagann et al.* [1983].

a scale height of 3 km. This nonnegligible sensitivity in the computed surface warming for these trace gases is largely because of the substantial difference in the stratospheric abundance between the uniform mixing-ratio profile and the profile with a 3-km scale height.

5.2. *Climatic Effects of the Projected Increases*

Figure 3 shows the results of the radiative-convective model calculations employing the projected increases shown in Tables 1*a* and 2. Our results basically confirm the suggestions by earlier calculations (see *World Meteorological Organization*, [1982*a*] for a summary) that the other trace gases can amplify the CO_2 surface warming by factors ranging from 1.5 to 3. But our results reveal several new features. We will summarize these features by considering the "best estimate" curve in Figure 3.

1. The surface warming (ΔT_g) due to all the trace gases (shown in Figure 3) is 1.54 K. The increase in CO_2 contributes about 0.71 K.
2. The CFC's, $CFCl_3$ (F11) and CF_2Cl_2 (F12), have the largest warming effect of all the trace gases besides CO_2. The direct radiative effect of $CFCl_3$ and CF_2Cl_2 (increase) contributes about 0.36 K to the surface warming. Furthermore, the stratospheric O_3 change, resulting largely from the projected increase in CFC's, leads to an additional warming of about 0.08 K. Hence the combined effect of 0.44 K due to CFC's is roughly 60% of the CO_2 effect.
3. Somewhat smaller, but nonnegligible, surface warming results from the increases in CH_4 (0.14 K), N_2O (0.1 K) and tropospheric O_3 (0.06 K).
4. Increases in $CHClF_2$ (F22), CH_3CCl_3, and CF_3Cl contribute, respectively, about 0.04 K, 0.02 K, and 0.01 K. All others shown in Figure 3 have negligible (<0.005 K) impact.

The warming we compute due to stratospheric ozone is at variance with *Wang et al.* [1980] results, who compute a surface cooling due to CFM-induced ozone perturbations. The major source of discrepancy is in the adopted stratospheric O_3 perturbation profile. The present profile is based on the most recent chemistry and reaction rates, and it shows that large decreases in middle and upper stratospheric O_3 profile are accompanied by somewhat smaller percentage increases in the lower stratosphere. Additional calculations were performed to examine the sensitivity of the computed surface warming to vertical distribution of O_3 change, which lead to the following inferences. The profile shown in Table 2 leads to a surface warming of 0.08 K. Roughly, 0.06 K is due to the O_3 decrease above 30 km, and the remainder of 0.02 K is due to the O_3 increase below 30 km. Thus the O_3 decrease above 30 km as well as the O_3 increase below 30 km contribute to a warming. The perplexing nature of this result can be understood from the detail analyses given by *Ramanathan et al.* [1976] and *Ramanathan and Dickinson* [1979], and hence only a brief discussion is given below.

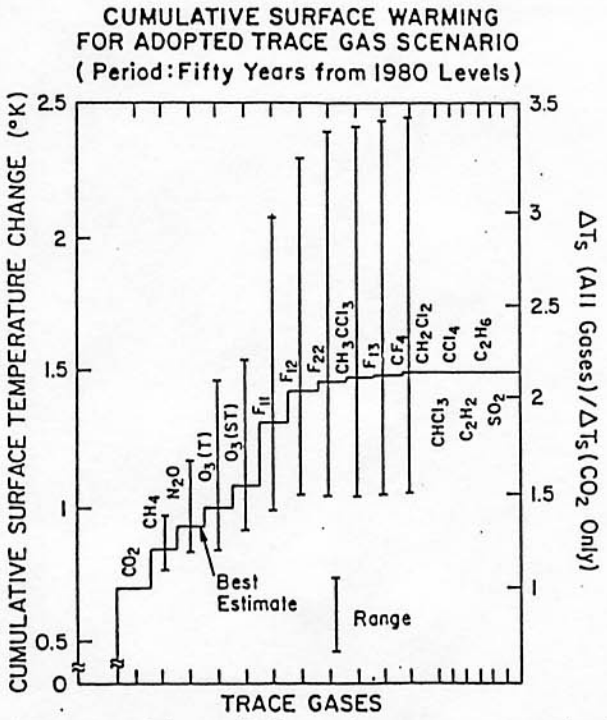

Fig. 3. Cumulative equilibrium surface temperature warming due to increase in CO_2 and other trace gases. Increases in gas amounts from 1980 values to 2030.

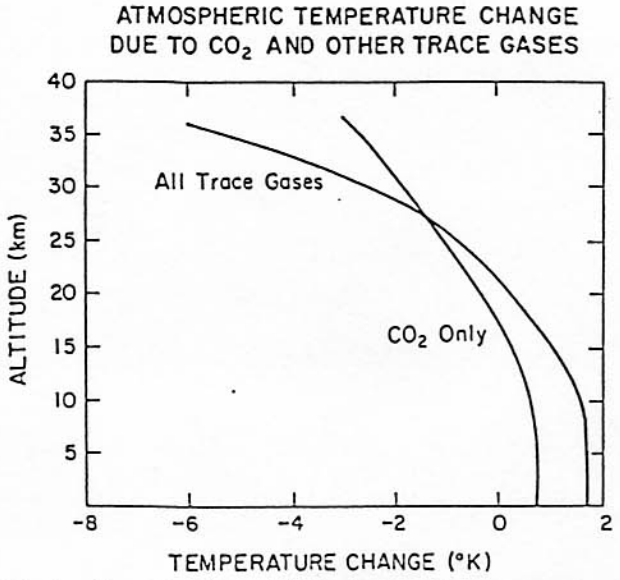

Fig. 4. Change in the vertical distribution of temperature due to an increase in CO_2 alone, and CO_2 along with all other trace gases listed in Figure 3. The trace gas increase scenario is as given by the "best estimate" values in Table 1*a*.

A decrease in stratospheric O_3, irrespective of the altitude of the decrease, would lead to an increase in the solar radiation reaching the troposphere, and this solar effect would tend to warm the surface. However, O_3 also alters the IR (longwave) emission from the stratosphere in two ways: first, the decreased solar absorption (due to O_3 decrease) cools the stratosphere; the cooler stratosphere emits less downward to the troposphere. Second, a decrease in O_3 reduces the absorption (by the O_3 9.6-μm band) of the surface-troposphere emission. This reduction causes an additional cooling of the stratosphere, which in turn, causes an additional reduction in the downward IR emission by the stratosphere. Thus the IR effects of O_3 decrease tend to cool the surface. However, the IR opacity of stratospheric CO_2, H_2O, and O_3 is sufficiently strong that the impact of the reduction in IR emission (by the stratosphere) on the surface diminishes with an increase in the altitude of O_3 perturbation. On the other hand, the surface warming induced by the solar effect is independent of the altitude of O_3 perturbation. Consequently, for a decrease in O_3 in the upper stratosphere, the solar effect dominates (leading to a surface warming), while for a decrease in the lower

TABLE 9. Gases Not Shown in Figure 3

Gas	7- to 13-μm Absorption Feature	Predicted Concentration Increase	Potential Role
$CHCl_2F$	band intensities unavailable	yes	yes
$C_2Cl_3F_3$	band intensities unavailable	yes	yes
$C_2Cl_2F_4$	band intensities unavailable	yes	yes
C_2ClF_5	band intensities unavailable	yes	yes
SO_2; CS_2; H_2S	strong	uncertain	no
COS; CS_2; H_2S	weak	no	no
CH_2ClCH_2Cl	strong	small	no
CH_3Cl	weak	no	no
C_2H_6; C_2H_4; C_3H_8	weak	uncertain	no
HCHO; CH_3CHO	weak	uncertain	no
CH_3F; CH_3Br; CH_3I	weak	uncertain	no
CH_2F_2	strong	uncertain	yes
CHF_3	very strong	uncertain	yes
$CBrF_3$	very strong	small	no
HNO_3	strong	small but uncertain	no
NO_x(NO, NO_2, NO_3, N_2O_5)	weak	uncertain	no
HCN	weak absorption	uncertain	no

The first four chlorofluorocarbon gases here could contribute significantly to future global warming because of the spectral positions of their absorption bands in the 7–13 μm atmospheric window region if their band-absorption intensities are large enough. For other gases, e.g., HCN and SO_2, their absorption bands are not strong enough to be significant at present or near-present atmospheric concentrations. For other gases such as C_2H_6 and CH_3F, we have too little information to be able to estimate future trends.

stratospheric O_3, the IR effect dominates (leading to a surface cooling).

The uncertainty in our computed surface warming due to stratospheric O_3 change is best illustrated by the following examples. The profile of O_3 change in Table 2 for altitude above 30 km when combined with 10% uniform O_3 decrease between 12 and 30 km leads to a surface warming of 0.02 K; whereas the same profile (as in Table 2) above 30 km when combined with a 10% uniform O_3 increase between 12 and 30 km leads to a surface warming of 0.1 K. In view of the high sensitivity of the computed temperature change to the vertical O_3 profile, our computed estimates for stratospheric O_3 change should be viewed with caution because such distributions would be influenced by atmospheric dynamics (whose effects are ignored in this analysis) and of course by remaining uncertainties in model chemistry.

The vertical distribution of the computed atmospheric temperature change is shown in Figure 4. It is clear from this figure that other trace gas effects on temperatures are comparable to CO_2 effects, not only for surface warming, but also for stratospheric cooling. The stratospheric cooling, to a large extent, results from the stratospheric O_3 reduction. The potential climatic effect of gases that are not explicitly discussed in Figure 3 is summarized in Table 9.

5.3. *Effects of the Inferred Trace Gas Increases From the Preindustrial to the Present Levels*

For the sake of discussion, the concentrations for the year 1880 are associated with the preindustrial levels, and these concentrations have been shown in Table 1*b*, while the observed 1980 concentrations are shown in Table 1*a*. The computed equilibrium temperature changes are shown in Table 10. The CO_2 increase causes a surface warming of 0.52 K, which is enhanced by 50% due to the increase in the other trace gases. The computed stratospheric cooling due to CO_2 increase is substantial, but that due to other gases is negligible. The computed stratospheric cooling would be larger had we included the effects of stratospheric O_3 decrease due to increases in CFC's. From Table 10*b*, which shows the contribution of the individual gases, it is seen that CH_4, tropospheric O_3, and CFC's are the largest contributors, next to CO_2, to the surface warming computed for the period 1880–1980.

6. SUMMARY

The basic conclusion that can be derived from the present study is that the radiative effects of increases in trace gases (other than CO_2) are as important as that of CO_2 increase in determining the climate change of the future or the past 100 years. Several tens of man-made chemicals have been detected in the troposphere and about 20 of these have strong absorption features in the 7- to 13-μm regions of the longwave spectrum. The present-day, taken as the year 1980, concentrations are taken from in situ observations. A careful analysis of the measured trends from early 1970's to 1980 form the basis for the concentrations projected 50 years into the future. Published ice-core CH_4 observations, surface-based O_3 observations, and other studies are used to infer the trace gas concentrations for the preindustrial era. The equilibrium surface and atmospheric temperature changes estimated with the aid of a radiative-convective model reveal the following features.

1. The preindustrial to present-day increase in CO_2 causes an equilibrium surface warming of 0.5 K in the model, which is enhanced by a factor of 1.5 by the increases in the other trace gases. CH_4, tropospheric O_3, and CFC's are the largest contributors to this enhancement. The upper stratospheric cooling due to the CO_2 increase is as large as about 3 K.

2. The projected CO_2 increase from 339 ppm in the year 1980 to 450 ppm in 2030 warms the model surface by 0.7 K, which is enhanced by a factor of about 2.1 by the other trace

gases. The factor of trace gas enhancement varies from about 1.5 to 3 depending on the assumed scenario. The trace gases that contribute to this significant enhancement are $CFCl_3$ (F11), CF_2Cl_2 (F12), CH_4, N_2O, stratospheric and tropospheric O_3. Somewhat smaller but nonnegligible contributions arise from $CHClF_2$ (F22), CH_3CCl_3, and $CFCl_3$.

3. The stratospheric O_3 changes resulting from the assumed increase in CFC's and other chlorine compounds by year 2030 are a large decrease in middle stratospheric O_3 accompanied by a slight increase in lower stratospheric O_3. Hence although CFC's are estimated to cause only a slight reduction in the column ozone, the significant perturbation to the shape of the O_3 profile leads to a nonnegligible surface warming of 0.08 K. Thus the O_3 change due to CFC's adds to the surface warming of 0.36 K resulting from the CFC direct radiative effects. These two effects when considered together make CFC's the largest contributors (next to CO_2) to the overall surface warming computed in this study. However, because of the strong sensitivity of the computed surface warming to the vertical profile of O_3 change, the magnitude of the potential surface warming due to stratospheric O_3 change is highly uncertain.

4. All of the other trace gases perturb the vertical atmospheric profile in the same manner as CO_2 in the following sense: they warm the surface and the troposphere while cooling the stratosphere (above 20 km) significantly. However, there is one important difference between the radiative effects of CO_2 and the other trace gases: as pointed out by *Dickinson et al.* [1978], CFC's have a strong warming on the tropical tropopause. Also the studies by *Ramanathan and Dickinson* [1979] and *Fels et al.* [1980] reveal the significant sensitivity of tropical tropopause to O_3 perturbations. Warming of the tropical tropopause by 2–3 K could lead to large changes in stratospheric water vapor.

5. On a ppb basis, CF_3Cl has the strongest greenhouse effect (exceeding very slightly even that of CFC12) followed closely by $CBrF_3$, CF_2Cl_2 (F12), CHF_3, $CFCl_3$ (F11), and C_2F_6 (F116), all of which have effects comparable to that of $CFCl_3$ or CF_2Cl_2. Gases such as CF_4, CCl_4, and PAN have strong absorption features, but due to the overlap with CH_4, N_2O, CO_2, and H_2O bands, these gases are not very effective in enhancing the atmospheric greenhouse effect. However, our conclusion concerning the overlap effects should be considered as tentative. Measurements of narrowband spectroscopic parameters for these other trace gases are currently not available, and such measurements are needed for improving the accuracy of the estimates for the overlap effects. For important species such as $C_2Cl_3F_3$ (F113), $C_2Cl_2F_4$ (F114), and C_2ClF_5 (F115) even band strengths are not available.

6. The accurate radiation model developed here for $CFCl_3$ (F11) and CF_2Cl_2 (F12) helped sort out the differences between the various published studies for the estimated surface warming.

TABLE 10. Computed Temperature Changes due to Inferred Trace Gases for the Period 1880–1980

Constituent	Temperature Change, K: Surface*	Stratosphere, km: 26–30	Stratosphere, km: 38–42
a. *Surface and Stratospheric Temperature Change*			
CO_2	0.52	−0.77	−2.78
CO_2 plus all other gases	0.79	−0.8	−2.85

Constituent	Concentration Change	Temperature Change
b. *Itemized Contribution to Surface Warming*		
CO_2	275–339 ppm	0.52
CH_4	1.15–1.65 ppm	0.12
N_2O	0.285–0.3 ppm	0.02
Troposphere O_3	12.5%	0.04
CFC11	0–0.18 ppb	0.025
CFC12	0–0.28 ppb	0.04
All others in Table 1*a*	0 to 1980 values	0.02

Possible changes in stratospheric O_3 are ignored.
*Surface air temperature change is larger than the surface temperature change by about 10–13%.

The important implication of this study is that the preindustrial to the present increase in CO_2 and the other trace gases might, very likely, have caused a significant perturbation to the radiative heating of the climate system. This perturbation radiative heating induces a warming of about 0.8 K in the present model, whereas it might have induced a warming twice as large in recent GCM's [*Washington and Meehl*, 1984; *Hansen et al.*, 1984]. These GCM's compute a 4 K global warming due to CO_2 doubling as opposed to the 2 K yielded by the radiative-convective model. The 0.8–1.6 K global warming, had it indeed occurred from the preindustrial to the present, should have been detectable above the statistical fluctuations of the climate. This is a controversial issue, and the published papers have contradictory results. *Hansen et al.* [1982] suggest that the CO_2 warming is discernible from observed records of global or hemispherical average temperatures. The statistical analysis of the 70-year homogeneous (in time and in longitude) temperatures for 50–70°N by *Madden and Ramanathan* [1980] has failed to reveal the CO_2 effect. Before we can attempt to verify the greenhouse theories of preindustrial to present warming by comparing model results with the observations, the following important issues must be dealt with.

1. The one-dimensional and GCM results pertain only to the equilibrium warming of the surface to a step-function increase in the trace gases. The quantity of interest, for the purpose of verification, is the transient climate response to a time-varying distribution of trace gases. Even assuming that time-dependent trace gas distribution is known (for the past 100 years), our understanding of the ocean mixed layer interactions with the atmosphere and the thermocline as well as the lateral ocean heat transport is too imprecise to estimate reliably the transient response of the climate system.

2. Other climate forcing terms, e.g., solar irradiance, volcanic aerosols, surface radiative properties, can also change on the time scales of interest to this study, and we do not have adequate data bases to estimate their contributions to past climates. Major volcanic events, such as El Chichon, can cause an equilibrium global cooling of 0.5–1 K, but the aerosol residence time is about 2 years or less, and as yet, we have not come to grips with the tough issue of estimating the transient response to an episodic forcing.

3. The last issue concerns the source of errors in observations of temperatures, humidities, and other trace gases arising from instrumental and sampling biases. There are no reliable global measurements for key components like lower stratospheric H_2O and tropospheric O_3.

It is hoped this study will provide more scientific justification for making some key measurements on a long-term

basis of trace gas trends (at least the top 12 gases identified here), stratospheric aerosols, stratospheric humidity, and tropical tropopause temperatures. Of equal importance, accurate measurements of narrow-band spectroscopic parameters and band strengths for the trace gases are urgently needed.

Acknowledgments. We are indebted to Dr. Niki for providing unpublished data. One of us (V.R.) thanks the Atmospheric Sciences Division, NASA Langley for the hospitality extended during the sabbatical visit. L. B. Callis of NASA Langley provided a careful review of an earlier version of this manuscript. We thank Gretchen Escobar for typing several versions of this manuscript. We also thank M. Coffey of NCAR for providing the routines and data tapes for inferring narrow-band model parameters. NCAR is sponsored by the National Science Foundation.

REFERENCES

Alexandrov, E. L., J. L. Konol, A. Ch. Khrgian, L. R. Rakipova, and Yu. S. Sedonov, Contribution of ozone and other minor trace gases to atmospheric radiation regime and their possible effect on global climate change, WMO Global Ozone Res. and Monitoring Proj. Rep. 10, 79 pp., World Meteorol. Organ., Geneva, 1981.

Andreae, M. O., and H. Raemdonck, Dimethyl sulfide in the surface ocean and the marine atmosphere: A global view, *Science, 221*, 744–747, 1983.

Angell, J. K., and J. Korshover, Global variation in total ozone and layer-mean ozone: An update through 1981, *J. Climate Appl. Meteorol., 22*, 1611–1627, 1983.

Bauer, E., A catalog of perturbing influences on stratospheric ozone 1955–1975, *J. Geophys. Res., 84*, 6929–6940, 1979.

Berg, W. W., L. E. Heidt, W. Pollock, P. D. Sperry, R. J. Cicerone, and E. S. Gladney, Brominated organic species in the Arctic atmosphere, *Geophys. Res. Lett., 11*, 429–432, 1984.

Blake, D. R., E. W. Mayer, S. C. Tyler, Y. Makide, D. C. Montague, and F. S. Rowland, Global increase in atmospheric methane concentrations between 1978 and 1980, *Geophys. Res. Lett., 9*, 477–480, 1982.

Bojkov, R. D., Tropospheric ozone, its changes and possible radiative effect, *WMO Spec. Environ. Rep. 16*, World Meteorol. Organ., Geneva, 1983.

Boughner, R. E., and V. Ramanathan, Climatic consequences of increasing CO_2: A study of the feedback mechanisms between increased CO_2 concentrations and the atmospheric ozone, water vapor, and thermal structure and balance, paper presented at the Second Conference on Atmospheric Radiation, Am. Meteorol. Soc., Arlington, Va., Oct. 29–31, 1975.

Callis, L. B., M. Natarajan, and R. E. Boughner, On the relationship between the greenhouse effect, atmospheric photochemistry, and species distributions, *J. Geophys. Res., 88*, 1401–1426, 1983.

Cess, R. D., The optically thin approximation, Meeting of Experts on Potential Climatic Effects of Ozone and Other Trace Gases, *WMO Rep. 14*, pp. 27–28, World Meteorol. Organ., Geneva, 1982.

Chamberlain, J. W., H. M. Foley, G. J. MacDonald, and M. A. Rudenman, Climatic effects of minor atmospheric constituents, in *Carbon Dioxide Review: 1982*, edited by W. C. Clark, pp. 253–278, Clarendon Press, New York, 1982.

Chatfield, R. B., and H. Harrison, Tropospheric ozone, 2, Variations along a meridional band, *J. Geophys. Res., 82*, 5969–5976, 1977.

Chemical Manufacturers Association, 1982 world production and sales of fluorocarbons FC-11 and FC-12, 29 pp., Washington, D. C., 1983.

Cicerone, R. J., Atmospheric carbon tetrafluoride: A nearly inert gas, *Science, 206*, 59–61, 1979.

Cicerone, R. J., and R. Zellner, The atmospheric chemistry of hydrogen cyanide, *J. Geophys. Res., 88*, 10689–10696, 1983.

Cicerone, R. J., S. Walters, and S. C. Liu, Nonlinear response of stratospheric ozone column to chlorine injections, *J. Geophys. Res., 88*, 3647–3661, 1983.

Craig, H., and C. C. Chou, Methane: The record in polar ice cores, *Geophys. Res. Lett., 9*, 1221–1224, 1982.

Crutzen, P. J., and L. T. Gidel, A two-dimensional photochemical model of the atmosphere, 2, The tropospheric budgets of the anthropogenic chlorocarbons, CO, CH_4, CH_3Cl and the effect of various NO_x sources on tropospheric ozone, *J. Geophys. Res., 88*, 6641–6661, 1983.

Cunnold, D., R. Prinn, R. Rasmussen, P. Simmonds, F. Alyea, C. Cardelino, A. Crawford, P. Fraser, and R. Rosen, The Atmospheric Lifetime Experiment, 3, Lifetime methodology and application to 3 years of $CFCl_3$ data, *J. Geophys. Res., 88*, 8379–8400, 1983*a*.

Cunnold, D., R. Prinn, R. Rasmussen, P. Simmonds, F. Alyea, C. Cardelino, and A. Crawford, The Atmospheric Lifetime Experiment, 4, Results for $CFCl_2$ based on 3 years of data, *J. Geophys. Res., 88*, 8401–8414, 1983*b*.

Dickinson, R. E., Modeling climatic changes due to carbon dioxide increases, in *Carbon Dioxide Review*, edited by W. C. Clark, pp. 101–133, Clarendon Press, New York, 1982.

Dickinson, R. E., S. C. Liu, and T. M. Donahue, Effect of clorofluoromethane infrared radiation on zonal atmospheric temperature, *J. Atmos. Sci., 35*, 2142–2152, 1978.

Donner, L., and V. Ramanathan, Methane and nitrous oxide: Their effects on the terrestrial climate, *J. Atmos. Sci., 37*, 119–124, 1980.

Duxbury, J. M., D. R. Baldwin, R. E. Terry, and R. L. Tate, Emissions of nitrous oxide from soils, *Nature, 298*, 462–464, 1982.

Ehhalt, D. H., R. J. Zander, and R. A. Lamontagne, On the temporal increase of tropospheric CH_4, *J. Geophys. Res., 88*, 8442–8446, 1983.

Fabian, P., R. Borchers, D. Gomer, and S. A. Penkett, The vertical distribution of halocarbons in the stratosphere, Quadrennial Ozone Symposium, IAMAP Programs and Abstracts, pp. 3–6, Int. Assoc. of Meteorol. and Atmos. Phys., 1984.

Fels, S. B., J. D. Mahlman, M. D. Schwarzkopf, and R. W. Sinclair, Stratospheric sensitivity to perturbations in ozone and carbon dioxide: Radiative and dynamical response, *J. Atmos. Sci., 37*, 2265–2297, 1980.

Fenical, W., Natural products chemistry in the marine environment, *Science, 215*, 923–928, 1982.

Fishman, J., V. Ramanathan, P. J. Crutzen, and S. C. Liu, Tropospheric ozone and climate, *Nature, 282*, 818–820, 1979*a*.

Fishman, J., S. Solomon, and P. J. Crutzen, Observational and theoretical evidence in support of a significant in-situ photochemical source of tropospheric ozone, *Tellus, 31*, 432–446, 1979*b*.

Goldman, A., F. S. Bonomo, and D. G. Murray, Statistical band model analysis and integrated intensity for the 11.8 μm band of $CFCl_3$, *Appl. Opt., 15*, 2305–2307, 1976*a*.

Goldman, A., F. S. Bonomo, and D. G. Murray, Statistical band model analysis and integrated intensity for the 10.8 μm band of CF_2Cl_2, *Geophys. Res. Lett., 3*, 309–312, 1976*b*.

Goldman, A., D. G. Murray, F. J. Murray, G. R. Cook, J. W. Van Allen, F. S. Bonomo, and R. D. Blatherwick, identification of the ν_3 vibration-rotation band of CF_4 in balloon-borne infrared solar spectra, *Geophys. Res. Lett., 6*, 609–612, 1979.

Hameed, S., R. D. Cess, and J. Hogan, Response of the global climate to changes in atmospheric chemical composition due to fossil fuel burning, *J. Geophys. Res., 85*, 7537–7545, 1980.

Hansen, J. E., A. Lacis, and S. A. Lebedeff, Commentary on climatic effects of minor atmospheric constituents, in *Carbon Dioxide Review: 1982*, edited by W. C. Clark, pp. 284–286, Clarendon Press, New York, 1982.

Hansen, J. E., A. Lacis, D. Rind, G. Russell, P. Stone, I. Fung, R. Ruedy, and J. Lerner, Climate sensitivity: Analysis of feedback mechanisms, in *Climate Processes and Climate Sensitivity, Maurice Ewing Ser. 5*, edited by J. E. Hansen and T. Takahashi, AGU, Washington, D. C., 1984.

Herranz, J. R. de la Cierva, and J. Morcillo, Intensidades absolutas en infrarrojo de bandes fundamentales del fluoroformo, chloroformo, trifluorclorometano y trichlorofluormetano, *An. R. Soc. Esp. Fis. Quim. Madrid, A55*, 69–76, 1959.

Herrmann, J., and W. Jaeschke, Measurements of H_2S and SO_2 over the Atlantic Ocean, *J. Atmos. Chem., 1*, 111–124, 1984.

Hummel, J. R., and R. A. Reck, The direct thermal effects of $CHClF_2$, CH_3CCl_3 and CH_2Cl_2 on atmospheric surface temperatures, *Atmos. Environ., 15*, 379–382, 1981.

Kagann, R. H., J. W. Elkins, and R. L. Sams, Absolute band strengths of halocarbons F-11 and F-12 in the 8- to 16-μm region, *J. Geophys. Res., 88*, 1427–1432, 1983.

Karol, I., et al., Atmospheric ozone and global climate, Report of U.S./USSR Workshop on the Climatic Effects of Increased Atmospheric Carbon Dioxide, Leningrad, 1981.

Kiehl, J. T., and V. Ramanathan, CO_2 radiative parameterization used in climate models: Comparison with narrow band models and with laboratory data, *J. Geophys. Res., 88*, 5191–5202, 1983.

Kley, D., J. W. Drummond, M. McFarland, and S. C. Liu, Tropospheric profiles of NO_x, *J. Geophys. Res., 86*, 3153–3161, 1981.

Lacis, A., J. Hansen, P. Lee, T. Mitchell, and S. Lebedeff, Greenhouse

effect of trace gases, 1970–1980, *Geophys. Res. Lett.*, *8*, 1035–1038, 1981.
Levy, H., J. D. Mahlman, W. J. Moxim, and S. C. Liu, Tropospheric ozone: The role of transport, *J. Geophys. Res.*, in press, 1985.
Liu, S. C., D. Kley, M. McFarland, J. D. Mahlman, and H. Levy II, On the origin of tropospheric ozone, *J. Geophys. Rev.*, *85*, 7546–7552, 1980.
Logan, J. A., Trends in tropospheric ozone, paper presented at Second Symposium on the Composition of the Nonurban Troposphere, Williamsburg, Va., May 1982.
Logan, J. A., M. J. Prather, S. C. Wofsy, and M. A. McElroy, Atmospheric chemistry: Response of human influence, *Philos. Trans. R. Soc. London*, *290*, 187–234, 1978.
Logan, J. A., M. J. Prather, S. C. Wofsy, and M. B. McElroy, Tropospheric chemistry: A global perspective, *J. Geophys. Res.*, *86*, 7210–7254, 1981.
Lovelock, J. E., Natural halocarbons in air and in sea, *Nature*, *256*, 193–194, 1975.
Madden, R. A., and V. Ramanathan, Detecting climate change due to increasing carbon dioxide, *Science*, *209*, 763–768, 1980.
Manabe, S., and R. T. Wetherald, Thermal equilibrium of the atmosphere with a given distribution of relative humidity, *J. Atmos. Sci.*, *24*, 241–259, 1967.
Maroulis, P. J., A. L. Torres, A. B. Goldberg, and A. R. Bandy, Atmospheric SO_2 measurements on Project Gametag, *J. Geophys. Res.*, *85*, 7345–7349, 1980.
McClatchey, R. A., et al., AFCRL atmospheric absorbtion line parameters compilation, *AFCRL-TR-73-0096*, 77 pp., Air Force Cambridge Res. Lab., Hanscom Field, Bedford, Mass., 1973.
Nanes, R., P. M. Silvaggio, and R. W. Boese, Temperature dependence of intensities of the 8-12 μm bands of $CFCl_3$, *J. Quant. Spectros. Radiat. Transfer*, *23*, 211–220, 1980.
National Academy of Sciences/National Research Council, Halocarbons: Effects on stratospheric ozone, Washington, D. C., 1976.
National Academy of Sciences/National Research Council, Stratospheric ozone depletion by halocarbons: Chemistry and transport, Washington, D. C., 1979.
National Academy of Sciences/National Research Council, Causes and effects of stratospheric ozone reduction: An update, National Academy Press, Washington, D. C., 1982.
National Aeronautics and Space Administration, The stratosphere: Present and future, *NASA Ref. Publ. 1049*, 1979.
National Research Council, Carbon dioxide and climate: A second assessment, Report of the CO_2/Climate Review Panel, National Academy Press, Washington, D. C., 1982.
National Research Council, Changing climate, Report of the Carbon Dioxide Assessment Committee, National Academy Press, Washington, D. C., 1983.
Penkett, S. A., Nonmethane organics in the remote troposphere, in *Atmospheric Chemistry*, pp. 329–355, Springer, New York, 1982.
Penkett, S. A., N. J. D. Prosser, R. A. Rasmussen, and M. A. K. Khalil, Atmospheric measurements of CF_4 and other fluorocarbons containing the CF_3 grouping, *J. Geophys. Res.*, *86*, 5172–5178, 1981.
Prather, M. J., M. B. McElroy, S. C. Wofsy, Reductions in ozone at high concentrations of stratospheric halogens, *Nature*, *312*, 227–231, 1984.
Pugh, L. A., and K. N. Rao, Intensities from infrared spectra, *Mol. Spectros., Mod. Res.*, *2*, 165–225, 1976.
Ramanathan, V., Greenhouse effect due to chlorofluorocarbons: Climatic implications, *Science*, *190*, 50-52, 1975.
Ramanathan, V., The role of ocean-atmospheric interactions in the CO_2 climate problem, *J. Atmos. Sci.*, *38*, 918–930, 1981..
Ramanathan, V., Commentary on climatic effects of minor atmospheric constituents, in *Carbon Dioxide Review: 1982*, edited by W. C. Clark, Clarendon Press, New York, 1982.
Ramanathan, V., and J. A. Coakley, Climate modeling through radiative-convective models, *Rev. Geophys. Space Phys.*, *16*, 465–489, 1978.
Ramanathan, V., and R. E. Dickinson, The role of stratospheric ozone in the zonal and sesonal radiative energy balance of the earth-troposphere system, *J. Atmos. Sci.*, *36*, 1084–1104, 1979.
Ramanathan, V., L. B. Callis and R. E. Boughner, Sensitivity of atmospheric and surface temperature to perturbations in stratospheric concentration of ozone and nitrogen-dioxide, *J. Atmos. Sci.*, *33*, 1092-1112, 1976.
Rasmussen, R. A., and M. A. K. Khalil, Atmospheric methane: Trends and seasonal cycles, *J. Geophys. Res.*, *86*, 9826–9832, 1981.
Rasmussen, R. A., L. E. Rasmussen, M. A. K. Khalil, and R. W. Dalluge, Concentration distribution of methyl chloride in the atmosphere, *J. Geophys. Res.*, *85*, 7350–7356, 1980.
Reck, R. A., and D. L. Fry, The direct effects of chlorofluoromethanes on the atmospheric surface temperature, *Atmos. Environ.*, *12*, 2501–2503, 1978.
Revelle, R. R., Methane hydrates in continental slope sediments and increasing atmospheric carbon dioxide, in *Changing Climate*, sect. 3.5, pp. 252–261, National Academy of Sciences, Washington, D. C., 1983.
Rothman, L. S., and R. R. Gamache, A. Barbe, A. Goldman, J. R. Gillis, L. R. Brown, R. A. Toth, J. M. Flaud, and C. Camy-Peyret, AFGL atmospheric absorption line parameters compilation: 1982 edition, *Appl. Opt.*, *15*, 2247–2256, 1983.
Rotty, R. M., and G. Marland, Constraints on carbon dioxide production from fossil fuel use, paper presented at the Energy/Climate Interactions Workshop, Munster, Germany, March 3–8, 1980.
Rudolph, J., and D. H. Ehhalt, Measurements, of C_2-C_5, hydrocarbons over the North Atlantic, *J. Geophys. Res.*, *86*, 11959-11964, 1981.
Saeki, S., M. Mizumo, and S. Kondo, Infrared absorption intensities of methane and fluoromethanes, *Spectrochim. Acta Part A*, *32*, 403–413, 1976.
Simmonds, P. G., F. N. Alyea, C. A. Cardelino, A. J. Crawford, D. M. Cunnold, B. C. Lane, J. E. Lovelock, R. G. Prinn, and R. A. Rasmussen, The Atmospheric Lifetime Experiment, 6, Results for carbon tetrachloride based on three years data, *J. Geophys. Res.*, *88*, 8427–8441, 1983.
Singh, H. B., and L. J. Salas, Peroxyacetyl nitrate in the free troposphere, *Nature*, *302*, 326–328, 1983.
Singh, H. B., D. P. Fowler, and T. O. Peyton, Atmospheric carbon tetrachloride: Another manmade pollutant, *Science*, *192*, 1231–1234, 1976.
Singh, H. B., L. J. Salas, and R. E. Stiles, Selected man-made halogenated chemicals in the air and oceanic environment, *J. Geophys. Res.*, *88*, 3675–3683, 1983*a*.
Singh, H. B., L. J. Salas, and R. E. Stiles, Methyl halides in and over the eastern Pacific (40°N–32°S), *J. Geophys. Res.*, *88*, 3684–3690, 1983*b*.
Smagorinsky, J., Effects of carbon dioxide, chap. 4, sect. 4.1, in *Changing Climate*, pp. 266–284, Report of the Carbon Dioxide Assessment Committee, National Research Council, 1983.
Sparrow, E. M., and R. D. Cess, *Radiation Heat Transfer*, 366 pp., McGraw-Hill, New York, 1970.
Surgeon General, Health effects of toxic pollutants: A report from the Surgeon General, Report prepared for U.S. Senate, Department of Health and Human Services, *Serial 96-15*, Washington, D. C., 1980.
Turco, R. P., R. C. Whitten, O. B. Toon, J. B. Pollack, and P. Hamill, OCS, Stratospheric aerosols and climate, *Nature*, *283*, 283–286, 1980.
Varanasi, P., and F. K. Ko, Intensity measurements in freon bands of atmospheric interest, *J. Quant. Spectros. Radiat. Transfer*, *17*, 385–389, 1977.
Volz, A., D. H. Ehhalt, and R. G. Derwent, Seasonal and latitudinal variation of ^{14}CO and the tropospheric concentrations of OH radicals, *J. Geophys. Res.*, *86*, 5163–5171, 1981.
Wang, W. C., Ozone changes: Climatological effects, in *Stratospheric Ozone and Man*, edited by F. A. Bower and R. B. Ward, pp. 123–135, CRC Press, Cleveland, Ohio, 1982.
Wang, W. C., Y. L. Yung, A. A. Lacis, T. Mo, and J. E. Hansen, Greenhouse effect due to manmade perturbations of trace gases, *Science*, *194*, 685–690, 1976.
Wang, W. C., J. P. Pinto, and Y. L. Yung, Climatic effects due to halogenated compounds in the earth's atmosphere, *J. Atmos. Sci.*, *37*, 333–338, 1980.
Washington, W. M., and G. A. Meehl, Seasonal cycle experiment on the climate sensitivity due to a doubling of CO_2 with an atmospheric general circulation model coupled to a simple mixed layer model, *J. Geophys. Res.*, *89*, 9475, 1984.
Weiss, R. F., The temporal and spatial distribution of tropospheric nitrous oxide, *J. Geophys. Res.*, *86*, 7185–7195, 1981.
Wine, P. H., W. L. Chameides, and A. R. Ravishankara, Potential role of CS_2 oxidation in tropospheric sulfur chemistry, *Geophys. Res., Lett.*, *8*, 543–546, 1981.
Wiscombe, W., and J. Evans, Exponential-sum fitting of radiative transmission functions, *J. Comp. Physiol.*, *24*, 416–444, 1977.
World Meteorological Organization, Report of the meeting of experts on potential climatic effects of ozone and other minor trace gases,

WMO Global Ozone Res. and Monitoring Prof. Rep. 14, 35 pp., Geneva, 1982*a*.

World Meteorological Organization, The stratosphere 1981—Theory and measurements, *WMO Rep. 11*, Geneva, 1982*b*.

World Meteorological Organization, The world climate research program report on the meeting of experts on detection of possible climate change, *WCP 29*, edited by W. W. Kellogg and R. D. Bojkov, p. 42, Geneva, 1983.

Wuebbles, D. J., Scenarios for future anthropogenic emissions of trace gases in the atmosphere, *UCID-18997*, Lawrence Livermore Lab., Berkeley, Calif., 1981.

Wuebbles, D. J., A theoretical analysis of the past variations in global atmospheric composition and temperature structure, Ph.D. thesis, *UCRL-53423*, Univ. of Calif., Davis, 1983*a*.

Wuebbles, D. J., Chlorocarbon emission scenarios: Potential impact on stratospheric ozone, *J. Geophys. Res.*, *88*, 1433–1440, 1983*b*.

R. J. Cicerone, J. T. Kiehl, and V. Ramanathan, National Center for Atmospheric Research, P. O. Box 3000, Boulder, CO 80307.

H. B. Singh, SRI International, Menlo Park, CA 94025.

(Received August 15, 1984;
revised January 14, 1985;
accepted January 18, 1985.)